IDŐJÁRÁS

QUARTERLY JOURNAL
OF THE HUNGARIAN METEOROLOGICAL SERVICE

CONTENTS

VOL. 97 * NO. 2 * APRIL–JUNE 1993

IDŐJÁRÁS

Quarterly Journal of the Hungarian Meteorological Service

Editor-in-Chief
E. MÉSZÁROS

Editor
T. TÄNCZER

Technical Editor
Mrs. M. ANTAL

Editorial Office: P.O. Box 39, H–1675 Budapest

Subscription from customers in Hungary should be sent to the Financial Department of the Hungarian Meteorological Service Kitaibel Pál u. 1, 1024 Budapest. The subscription rate is HUF 2000.

Abroad the journal can be purchased from the distributor: KULTURA, P.O. Box 149, H–1389 Budapest. The annual subscription rate is USD 56.

IDŐJÁRÁS

Quarterly Journal of the Hungarian Meteorological Service
Vol. 97, No. 2, April–June 1993

The dynamics of a shallow-water flow over topography Part I. Theory

I. Szunyogh

Department of Meteorology, Eötvös Loránd University,
Ludovika tér 2, H-1083 Budapest, Hungary

(Manuscript received 29 April 1993)

Abstract—Conservative quantities play an important role in the long-term behaviour of dynamical systems. This statement is especially valid for the so-called Casimir invariants, since the number of these quantities are infinite for the infinite-dimensional continuous Hamiltonian fluid dynamical systems. The appropriate form of Casimir invariants for motion in a homogeneous fluid with free surface is $C=\int\int hC(q)dxdy$ for any function C, even if the governing differential equations contain the effects of steep topography. Here q is the (absolute) potential vorticity and h is the vertical extent of a fluid column above the bottom surface. According to the above conservation laws, if h is a bounded quantity the statistical mechanics of a shallow-water flow are controlled by the quasi-conservation of $C=\int\int C(\zeta)dxdy$, for any function C of the relative vorticity ζ.

If the applied mathematical approximation conserves the energy, the discretized governing equations define a finite-dimensional quasi-Hamiltonian system which for the conservation laws can be investigated as for a finite-dimensional Hamiltonian system. In this paper using the quasi-Hamiltonian representation it has been shown, that the discretized equations provide the formal invariance only for a finite group of the discretized Casimir invariants (generally for the potential enstrophy and for the circulation), which yield the increasing sensitivity of the discretized equations to the high-frequency perturbations.

Key-words: Casimir invariants, finite-dimensional quasi-Hamiltonian structure, potential vorticity, rotational and divergent kinetic energy spectra.

1. Introduction

The time evolution of a dynamical system is constrained by the invariants of motion. It follows that the stability properties and the statistical mechanics of a fluid system are principally governed by the acting conservation laws.

For a given system of equations the conserved quantities can be classified into two groups. The first one consists of those invariants whose conservation

is formally provided by the governing equations. The other group contains the quasi-conserved quantities which are formally not, but approximately invariant for a given period of time using realistic initial conditions. In this period the stability and the statistical mechanics of the flow are practically controlled by the quasi-conserved quantities, while the time evolution of the meteorological fields is governed by the original system of equations.

It is clear that the quasi-conserved quantities are the formal invariants of the reduced system of equations, which can be derived from the original equations using the method of scale-analysis and the principle of consistency (or, in other words, the simplified system has to preserve all conservation laws of the original system). Accordingly, when examining the statistical mechanics and the stability properties of a given hydrodynamical system, it is necessary to identify the formal invariants for the original system and for its possible simplified versions.

The most efficient way to derive energy consistent reduced systems and examine their conservation laws is using the Hamiltonian formalism in symplectic notation (*Salmon*, 1983, 1988; *Shepherd*, 1990). Therefore, in the latest time the Hamiltonian formalism has an extensive role in the investigation of the stability properties (*Shepherd*, 1992), as well as in studying of statistical mechanical features of fluid mechanical systems.

It must be stated that the role and importance of each conservation law are different. For example, nowadays it is clear that the formal conservation of vorticity-type invariants plays a more important role in the actual conservation of energy (kinetic energy) than the formal conservation of the energy (kinetic energy) itself. Moreover, there are some additional problems in the case of the discretized equations. First of all, the applied discretization techniques can lead to the violation of the formal invariants of the original equations, which follows that these approximations cannot provide the conservation of all quasi-conserved quantities. Strictly speaking, the stability and the statistical mechanics of the discretized equations are principally governed by the conservative properties of the approximating equations. In this way, the identification of conserved quantities for the discretized equations has a great importance in examining the statistical mechanics of the system. An elegant and systematic way to identify these discretized invariants is the use of the quasi-Hamiltonian formalism of the discretized equations (*Szunyogh*, 1993). However, there are two necessary conditions of the applicability of this method. The approximated continuous system has to be a Hamiltonian one and the numerical schemes may not mix the approximations of the time and the spatial derivatives, as, for example, a semi-Lagrangian technique does.

In this paper the shallow-water system of equations containing the effect of bottom topography is considered as an original system of equations. For this system the quasi-conserved quantities are the formal invariants of the two-dimensional vorticity equations, namely the kinetic energy and the enstrophy.

It will be shown very clearly that the conservation of the formal vorticity-type invariants for the shallow-water equations is a necessary condition for the quasi-conservation of the enstrophy which provide the actual conservation of the kinetic energy.

The structure of the paper is as follows: *Section 2* is a short review of the Hamiltonian theory, while in *Section 3* the quasi-Hamiltonian formalism for fluid dynamical equations is described. In *Section 4* the role of the two-dimensional invariants are highlighted. In order to investigate the formal invariants of the shallow-water flow over steep topography, the governing equations are written in Hamiltonian form in *Section 5*. The role of the so-called Casimir invariants are examined in details in *Section 6*. *Section 7* concludes several remarks about the possible extensions. Finally, it should be mentioned that the subsequent part of this paper presents the result of a sequence of numerical experiments which were carried out with a well-known shallow-water model.

2. Hamiltonian structure in continuous model equations

In the symplectic notation the continuous model system can be represented by the equation

$$\boldsymbol{u}_t = J\frac{\delta H}{\delta \boldsymbol{u}}, \tag{1}$$

where $\boldsymbol{u}_t$ is the partial derivative of the prognostical vector variable $\boldsymbol{u}$ with respect to t, $H(\boldsymbol{u}(t))$ is the Hamiltonian function (generally the total energy) and J is a skew-symmetric transformation. In addition, the symplectic operator J satisfies the Jacobi condition (*Shepherd*, 1990). The conservation of energy follows immediately from the skew-symmetry of J, since

$$\frac{dH}{dt} = \left(\frac{\delta H}{\delta \boldsymbol{u}}, \frac{\partial \boldsymbol{u}}{\partial t}\right) = \left(\frac{\delta H}{\delta \boldsymbol{u}}, J\frac{\delta H}{\delta \boldsymbol{u}}\right) = -\left(\frac{\delta H}{\delta \boldsymbol{u}}, J\frac{\delta H}{\delta \boldsymbol{u}}\right), \tag{2}$$

where (,) is the relevant inner product for the function space $\{\boldsymbol{u}\}$. The conservation laws related to explicit symmetries (momentum-type invariants and the energy itself) can be identified by the Noether-theory (*Shepherd*, 1990), but it must be stated that the number of these invariants is finite.

The other group of invariants is associated with the particular form of the operator J. These so-called Casimir invariants are the solutions C of

$$J\frac{\delta C}{\delta \boldsymbol{u}} = 0. \tag{3}$$

Conservation of these quantities follows from

$$\frac{dC}{dt} = \left(\frac{\delta C}{\delta u}, J\frac{\delta H}{\delta u}\right) = -\left(\frac{\delta H}{\delta u}, J\frac{\delta C}{\delta u}\right) = 0, \tag{4}$$

using the skew-symmetry of J and the condition (3).

It can be seen that the Casimir invariants C do not depend on the Hamiltonian itself and they can be isolated by examining the kernel of the operator J. One of the most important features of these quantities is, that their number is infinite and so they can provide a strong control for the infinite-dimensional fluid-dynamical systems.

3. Quasi-Hamiltonian structure in the discretized equations

If the applied mathematical approximation conserves the energy, the model system possesses a quasi-Hamiltonian structure (*Szunyogh*, 1993) and the time evolution of the discretized vector variable x is governed by the equation

$$\frac{dx}{dt} = J\frac{dE}{dx}, \tag{5}$$

where the function $E(x(t))$ defines the total energy of the model and J is a skew-symmetric matrix-operator. The quasi-Hamiltonian denomination of this system is originated in the fact that the operator J does not satisfy the Jacobi condition. As a main advantage of this formalism, the behaviour of the discretized system can be investigated as for a finite dimensional Hamiltonian system.

In this case the Casimir invariants are the solutions C of the equation

$$J\frac{dC}{dx} = 0. \tag{6}$$

Conservation of these quantities follows from

$$\begin{aligned}\frac{dC}{dt} = \frac{dC}{dx}\frac{dx}{dt} &= \sum_{i=1}^{n}\frac{\partial C}{\partial x_i}\frac{\partial x_i}{\partial t} = \sum_{i=1}^{n}\frac{\partial C}{\partial x_i}\sum_{j=1}^{n}J_{ij}\frac{\partial E}{\partial x_j} = \sum_{i=1}^{n}\sum_{j=1}^{n}\frac{\partial C}{\partial x_i}J_{ij}\frac{\partial E}{\partial x_j} \\ &= -\sum_{i=1}^{n}\sum_{j=1}^{n}\frac{\partial E}{\partial x_i}J_{ij}\frac{\partial C}{\partial x_j} = \frac{dE}{dx}J\frac{dC}{dx} = 0.\end{aligned} \tag{7}$$

However, there is an essential difference between the condition (3) and (6),

the Eq. (6) defines only a finite number of independent conserved quantities. In order to see this important property, it has to be taken into consideration that the gradient vector $\partial C/\partial \boldsymbol{x}$ is the solution $\boldsymbol{y}$ of the homogeneous linear system of equations

$$J\boldsymbol{y} = 0. \tag{8}$$

There are nontrivial solutions of Eq. (8) if

$$\det(J) = 0. \tag{9}$$

Since the matrix J is skew-symmetric if the number of rows (columns) of the matrix is odd, the solutions exist independently of the particular value of the matrix elements. On the other hand, if the number of rows (columns) is even, the existence of the solutions depends on the particular value of the elements J_{ij}. It follows that the applied discretizing scheme can provide the conservation of the Casimir invariants only for specially constructed matrix operators. In the case when $\det(J)=0$ the general solution is

$$\boldsymbol{y} = Y_{n-r}\,t, \tag{10}$$

where Y_{n-r} is a matrix containing the n-r particular solutions of the system, while the components of the vector $t=[t_1, t_2,..t_r]$ are arbitrary free parameters. All the other solutions differ from Eq. (10) only in a constant multiplier, thus these solutions do not define new variables in a physical meaning.

4. Role of the two-dimensional invariants

The simplest model equation which has a meteorological meaning is the two-dimensional vorticity equation. In the Hamiltonian formalism it can be written as

$$u = \zeta, \quad J = -\partial(\zeta,.), \quad H(\zeta) = \frac{1}{2}\int\int |\nabla\psi|^2\, dx\,dy, \tag{11}$$

where $\zeta(x,y,t)=\nabla^2\,\psi(x,y,t)$ is the vorticity, $\psi(x,y,t)$ is the stream function and ∂ is the two-dimensional Jacobian (*Shepherd*, 1990). The Hamiltonian function $H(\zeta)$ is equal to the total energy of the fluid which, in this case, is equivalent to the total rotational kinetic energy E_{rot} of the flow.

The Casimir invariants are defined by

$$C = \iint C(\zeta)\, dx dy, \tag{12}$$

for any function C of the vorticity ζ. The most important invariants are associated with $C(\zeta)=\zeta$ and $C(\zeta)=\zeta^2$ which express the conservation of the total circulation and the enstrophy.

Conservation of enstrophy, together with the conservation of kinetic energy, provide the unique phenomenology of a two-dimensional incompressible flow (*Kraichnan*, 1975; *Vallis*, 1992). It means that there is an indirect energy transfer from the small scales, as well as a direct enstrophy cascade to the small scales which leads to the particular stability of the quasi-two-dimensional atmospheric and oceanic structures. This special feature of two-dimensional turbulence follows from the fact that the average wave number

$$k_1^2 = \left(\frac{D}{2\pi}\right)^2 \frac{\iint \zeta^2\, dx dy}{E_{rot}} = \left(\frac{D}{2\pi}\right)^2 \frac{\iint k^2 E(k)\, dp\, dq}{\iint E(k)\, dp\, dq}, \tag{13}$$

is a conserved quantity due to the conservation of the enstrophy, and the rotational kinetic energy E_{rot}, if $\vec{k}=(p,q)$ is the two-dimensional wave number, while the flow is confined in a cyclic box of side D.

Using this fact, following the pioneering works of *Kraichnan* (1967, 1975), many authors investigated the statistical mechanics of two-dimensional turbulence on an energy-enstrophy hypersurface in the phase space. However, as it was pointed out by *Shepherd* (1990), and *Carnevale* and *Fredriksen* (1987) for an infinite-dimensional system, the trajectories of nonlinear stable solutions cannot fill the entire energy-enstrophy hypersurface due to the invariance of higher moments of the vorticity. This means that the necessary condition for the ergodicity does not hold (*Khinchin*, 1949) which restricts the applicability of the *Kraichnan's* classical theory.

Although the enstrophy and the rotational kinetic energy are exact formal invariants only for the two-dimensional incompressible and nondivergent flows, the particular stability of quasi-two-dimensional atmospheric structures shows that for the large scale atmospheric motions in a some days period the rotational kinetic energy and the enstrophy are quasi-conserved quantities.

The situation is fairly different for the model equations which usually do not conserve the higher moments, and so the trajectories may fill the entire energy-enstrophy hypersurface. It means that the parameters of the equilibrium solutions describe the stability properties of the applied mathematical approximation instead of the stability properties of the original system. For instance, the average wave number is a possible index number to measure the inclination of the stability of the truncated models to the nonlinear instability (*Szunyogh*, 1992).

5. *The infinite-dimensional form of the governing equations*

In the symplectic notation the governing equations for quasistatic motion in a homogeneous incompressible fluid over steep topography can be defined by

$$\boldsymbol{u} = (\vec{v},h)^T, \tag{14.a}$$

$$H(\vec{v},h) = \frac{1}{2}\int\int\left[h(|\vec{v}|^2 + \frac{1}{2}gh + 2gh_s)\right]dxdy, \tag{14.b}$$

$$J = \begin{bmatrix} 0 & q & -\partial_x \\ -q & 0 & -\partial_y \\ -\partial_x & -\partial_y & 0 \end{bmatrix}, \tag{14.c}$$

where the potential vorticity q is defined by

$$q = (f+\zeta)h^{-1}, \tag{15}$$

v is the horizontal velocity, f is the Coriolis parameter, $\zeta = \vec{k}\nabla\times\vec{v}$ the vorticity, g the gravitational acceleration, h_s the bottom surface height and h the vertical extent of a fluid column above the bottom surface (for further details see Appendix A).

The Casimir invariants are defined by

$$C = \int\int hC(q)dxdy \tag{16}$$

for some function $C(q)$. It is clear that Eq. (16) defines infinite number of conserved quantities, which provides infinite number of constraints for the shallow-water flows. The most important Casimirs are related to $C=1$, $C=q$ and $C=q$ associated with conservation of mass, conservation of circulation, and conservation of potential enstrophy, respectively.

6. *The role of the Casimir invariants*

For the shallow-water system of Eq. (14) the time evolution of the relative vorticity and the divergence $\delta(x,y,t)$ are governed by the equations

$$\frac{\partial \zeta}{\partial t} = -\nabla(\zeta + f)\vec{v}, \tag{17.a}$$

$$\frac{\partial \delta}{\partial t} = \vec{k}\nabla\times(\zeta + f)\vec{v} - \Delta\left(\Phi + \frac{\vec{v}}{2}\right)^2, \tag{17.b}$$

and

$$\vec{v} = \vec{v}_\psi + \vec{v}_\kappa = \vec{k}\times\nabla\Delta^{-1}\zeta + \nabla\Delta^{-1}\delta, \tag{18}$$

where $\vec{v}_\psi$ is the rotational and $\vec{v}_\kappa$ is the divergent part of the velocity vector. Eq. (18) shows that the kinetic energy (per unit mass) of a shallow-water flow can be separated into two terms,

$$E_{kin} = E_\psi + E_\kappa = \frac{1}{2}(\nabla\Delta^{-1}\zeta)^2 + \frac{1}{2}(\nabla\Delta^{-1}\delta)^2, \tag{19}$$

where E_ψ is the rotational and E_κ is the divergent kinetic energy. In this way, the time evolution of rotational and kinetic energy is governed by the equations

$$\frac{\partial}{\partial t}E_\psi = (\vec{v}_\psi \times \vec{k})\nabla\Delta^{-1}\frac{\partial \zeta}{\partial t} = f(\vec{v}_\psi, \vec{v}_\kappa), \tag{20.a}$$

and

$$\frac{\partial}{\partial t}E_\kappa = \vec{v}_\kappa\nabla\Delta^{-1}\frac{\partial \zeta}{\partial t} = f(\vec{v}_\psi, \vec{v}_\kappa, \Phi). \tag{20.b}$$

As it was pointed out by *Warn* (1986), the divergent part of the kinetic energy evolves toward an equipartition among the wave-modes, while the rotational part of the kinetic energy is constrained by the quasi-conservation of the enstrophy. However, there is an additional transfer between the rotational and the divergent part of the energy, as it can be seen from Eqs. (17) and (20). The numerical experiments indicate that in the final equilibrium most of the kinetic energy is accumulated at the divergent modes, but in the first period there is a fairly stable quasi-two-dimensional equilibrium (*Errico*, 1984).

In this paper only the first period is examined in details. According to Eq. (12) and Eq. (16) the

$$Z^{(n)} = \int\int \zeta^n dx dy, \tag{21.a}$$

$$Q^{(n)} = \iint hq^n dxdy = \frac{1}{2}\int \int h\left[\frac{f+\zeta}{h}\right]^n dxdy, \tag{21.b}$$

($n=1,2,\ldots$) quantities are Casimir invariants for the two-dimensional vorticity equation and the shallow-water equations, respectively. Let

$$h_{\max} = \text{maximum}\,[h(x,y,t)], \tag{22}$$

then

$$|Z^{(1)}| = |Q^{(1)} - fA|, \qquad A = \iint dxdy, \tag{23.a}$$

$$|Z^{(n)}| \le h_{\max}^{n-1} |Q^{(n)}| + \sum_{k=1}^{n} C_k |Z^{(n-k)}|, \tag{23.b}$$

$$C_k = \binom{n}{k} f^k, \quad \text{if } n \ge 2, \tag{23.c}$$

(for further details see Appendix B). It can be seen that the $|Z^{(n)}|$ is a bounded quantity, since the first term on the right-hand side of Eq. (23.b) is constant according to Eq. (16), while the second term is bounded due to the recursion itself. What the most important is, the quasi conservation of $|Z^{(n)}|$ is controlled by the invariants of the original shallow-water system and the time-dependent variable h.

It must be emphasized that the formal conservation of energy has no direct role in the control of the spectral distribution of kinetic energy. It follows that the bottom topography may have an influence only through the parameter h_{max}, since the parameter h_s appears only in the energy function.

It should be mentioned that in the most extreme case $h(x,y,t)$ is a constant function, and the last column and the last row can be eliminated from J in Eq. (14.c) and Eq. (14) is simplified into the two-dimensional vorticity equation, while the quantities $Z^{(n)}$ become exact invariants.

The inequality (23) is valid for the discretized version of the quantity (21.a) and (21.b), too, but the integration in space have to be replaced by summarization for the discretized variables. As a main difference, the discretized equations provide the formal invariance only for a finite group of the $|Q^{(n)}|$ quantities (generally for $n=2$), which yields the increasing sensitivity of the discretized equations to the high-frequency perturbation.

For the sake of deeper understanding of the previous statement, we examine the acting process in details. As a consequence of the orographic effects,

divergent kinetic energy flows into the system. This divergent energy evolves toward an equilibrium among the wave number-modes. This means that, after a given time period, the divergent energy appears at the higher wave numbers, even if it is pumped in at the lowest wave numbers. Simultaneously, there is a continuous energy transfer between the rotational and the divergent part of the kinetic energy. In this way, rotational kinetic energy arises at the higher wave numbers since the numerical model cannot control the higher moments of the vorticity according to Eq. (23). This process leads to the violation of the conservation of lower moments due to the very effective nonlinear interactions. At the end of this process the numerical model becomes unstable and the energy catastrophe is bound to happen.

The process described above in part is the natural behaviour of the shallow-water system, since the conservation of $Z^{(n)}$ can be violated as a consequence of the variation of $h_{\max}$, even if the conservation of $Q^{(n)}$ for any n is preserved. In the nature this process is controlled by the viscosity, which consumes the kinetic energy of the high-frequency velocity perturbations, proportionally to the square of the wave number. However, numerical experiments indicate, that a viscosity coefficient, which is large enough to control the time evolution of the numerical model, after a time period leads to the catastrophic decrease of the kinetic energy (*Sadourny*, 1975).

Summarizing, the quasi-conservation of discretized $| Z^{(n)} |$ depends on two effects. The first of these effects is the time variation of the potential vorticity $| Q^{(n)} |$ due to the numerical approximation of the spatial derivatives, and the other effect is the increase of $h_{\max}$ which is a result of the topography if the flow satisfies the balance condition

$$\operatorname{div} \vec{v} = 0 \quad \text{at} \quad t = 0. \tag{24}$$

7. Concluding remarks

In this paper the influence of the divergent process on the nonlinear instabilities has been investigated. If an additional time dependent variable is introduced a new type of instability occurs and the scheme of the potential vorticity will contain this new variable. However, for all of these systems of equations the enstrophy is a quasi-conserved quantity due to conservation of potential vorticity, which provides the control of the nonlinear instability for a limited time-interval.

Eq. (23) gives a very rough quantitative estimation for the spectral behaviour of the shallow-water models. In order to understand deeper the acting processes involved, a series of numerical experiments were carried out with a well-known quasi-Hamiltonian model which provides the conservation of potential vorticity. The results of these detailed spectral investigations are in a

good accordance with the theoretical considerations presented here and they are demonstrated in the subsequent part of this paper.

References

Carnevale, G.F. and *Frederiksen, J.S.*, 1987: Nonlinear stability and statistical mechanics of flow over topography. *J. Fluid Mech. 175*, 157-181.

Errico, R. M., 1984: The statistical equilibrium solution of a primitive equation model. *Tellus 36A*, 42-51.

Khinchin, A.I., 1949: *Mathematical Foundation of Statistical Mechanics*. Dover, New York.

Kraichnan, R.H., 1967: Inertial ranges in two-dimensional turbulence. *Phys. Fluids 10*, 1417-1423.

Kraichnan, R.H., 1975: Statistical dynamics of two-dimensional flow. *J. Fluid Mech. 67*, 155-175.

Salmon, R., 1983: New equations for nearly geostrophic flow. *J. Fluid Mech. 153*, 133-152.

Salmon, R., 1988: Hamiltonian fluid mechanics. *Ann. Rev. Fluid Mech. 20*, 225-256.

Sadourny, R., 1975: The dynamics of finite-difference models of the shallow-water equations. *J. Atmos. Sci. 32*, 680-689.

Shepherd, T.G., 1990: Symmetries, conservation laws, and Hamiltonian structure in geophysical fluid dynamics. *Adv. Geophys. 32*, 287-338.

Shepherd, T.G., 1992: Arnol'd stability applied to fluid flow: Successes and failures. In *Nonlinear Phenomena in Atmospheric and Oceanic Sciences* (eds.: *G.F. Carnevale* and *R.T. Pierrehumbert*). Springer-Verlag, New-York.

Szunyogh, I., 1992: Statistical mechanics of inviscid truncated models of two-dimensional incompressible flows. *Időjárás 96*, 22-31.

Szunyogh, I., 1993: Finite-dimensional quasi-Hamiltonian structure in simple model equations. *Meteorol. Atmos. Phys. 51* (in press).

Vallis, G.K., 1992: Problems and phenomenology in two-dimensional turbulence. In *Nonlinear Phenomena in Atmospheric and Oceanic Sciences* (eds.: *G.F. Carnevale* and *R.T. Pierrehumbert*). Springer-Verlag, New-York.

Warn, T., 1986: Statistical mechanical equilibria of the shallow water equations. *Tellus 38A*, 1-11.

APPENDIX A

The governing equations in the original Eulerian form can be written as

$$\frac{\partial \vec{v}}{\partial t} + q\vec{k}\times h\vec{v} + \nabla(K + \Phi) = 0, \qquad \text{(A.1)}$$

$$\frac{\partial h}{\partial t} + \nabla(h\vec{v}) = 0, \tag{A.2}$$

where the kinetic energy per unit mass is

$$K = \frac{1}{2}|\vec{v}|^2, \tag{A.3}$$

and the potential energy is

$$\Phi = g(h + h_s), \tag{A.4}$$

and $\vec{k}$ denotes the vertical unit vector. Therefore, the Hamiltonian functional which is equivalent to the total energy of the fluid is

$$H(\vec{v},h) = \frac{1}{2}\int\int(h|\vec{v}|^2 + gh^2 + 2ghh_s)\,dxdy. \tag{A.5}$$

If follows that

$$\frac{\delta H}{\delta \vec{v}} = h\vec{v}, \quad \frac{\delta H}{\delta h} = \frac{1}{2}|\vec{v}|^2 + gh + gh_2, \tag{A.6}$$

and

$$\begin{bmatrix} \frac{\partial u}{\partial t} \\ \frac{\partial v}{\partial t} \\ \frac{\partial h}{\partial t} \end{bmatrix} = \begin{bmatrix} 0 & q & -\partial_x \\ -q & 0 & -\partial_y \\ -\partial_x & -\partial_y & 0 \end{bmatrix} \begin{bmatrix} hu \\ hv \\ \frac{1}{2}|\vec{v}|^2 + g(h+h_s) \end{bmatrix}, \tag{A.7}$$

which is equivalent to Eq. (14).

Shepherd (1990) examined the similar shallow-water system. Although he did not take into account the influence of the bottom surface, the operator J in his paper was the same as (14.c) *Salmon* (1988) pointed out that if the Hamiltonian H has been modified alone, leaving the symplectic operator J undistributed, the energy conservation is satisfied due to the skew symmetry of J, and the Casimirs (which depend on J, not H) do not change. In this way Eq. (14) defines an energy conservative system, and its Casimirs (16) correspond to those which were derived by *Shepherd* (1990).

APPENDIX B

Using (21.a), definition of $Z^{(n)}$ is

$$\begin{aligned} |Z^{(n)}| &= \left|\iint \xi^n dx dy\right| = \left|\iint [(\xi+f)^n - g^{(n)}] dx dy\right| \leq \\ &\leq \left|\iint (\xi+f)^n dx dy\right| + \left|\iint g^{(n)} dx dy\right| \\ &\leq \left|\iint \left(\frac{h_{\max}}{h}\right)^{n-1} (\xi+f)^n dx dy\right| + \left|\iint g^{(n)} dx dy\right| \\ &= h_{\max}^{n-1} |Q^{(n)}| + \left|\iint g^{(n)} dx dy\right| . \end{aligned} \tag{B.1}$$

The $g^{(n)}$ can be derived from the Newtonian binomial form

$$\xi^n = (\xi+f)^n - \sum_{k=1}^{n} C_k \xi^{n-k}, \tag{B.2}$$

from which it follows that

$$g^{(n)} = \sum_{k=1}^{n} C_k \xi^{n-k}. \tag{B.3}$$

Using the (21.a) definition of $Z^{(n)}$ again

$$\begin{aligned} \left|\iint g^{(n)} dx dy\right| &= \left|\iint \left(\sum_{k=1}^{n} C_k \zeta^{n-k}\right) dx dy\right| = \left|\sum_{k=1}^{n} \iint C_k \zeta^{n-k} dx dy\right| \\ &= \left|\sum_{k=1}^{n} C_k Z^{(n-k)}\right| \leq \sum_{k=1}^{n} C_k |Z^{(n-k)}| . \end{aligned} \tag{B.4}$$

The Eq. (B.4), together with Eq. (B.1), gives the inequality (23).

IDŐJÁRÁS
Quarterly Journal of the Hungarian Meteorological Service
Vol. 97, No. 2, April–June 1993

Development of decision method for storm warning at Lake Balaton

I. Bartha

Storm Warning Observatory of Hungarian Meteorological Service
P.O. Box 80, H-8600 Siófok, Hungary

(Manuscript received 4 March 1993; in final form 16 June 1993)

Abstract—Weather warnings are of great importance in respect to protection of life and property. The Storm Warning Observatory at Lake Balaton was founded with the aim of providing warnings 1–2 hours earlier for the holiday-makers on the expected wind gusts exceeding 12 or 17 m/s. As a result of successive investigations an objective decision procedure has been elaborated in which weather radar data are also used. This procedure can be executed interactively on a computer. It combines the method based on conventional data with the approach of using radar information.

As a development, the permanence of wind-hazardous degrees was investigated during frontal and convective weather situations. For the purpose of our investigations, radar and synoptic observational data were used. The determined distribution functions of empirical probability for the permanence of wind-hazardous degrees associated with Cb-clouds can be used for the further optimization of the decision method.

Key-words: Cb-cloud, wind-hazard, wind gust estimation, nowcasting, decision procedure, very short range forecast.

1. Introduction

Stormy wind is one of the most dangerous weather phenomena in the region of Lake Balaton. In respect to protection of life and property the weather warnings are of great importance to the holiday-makers, sailors and surf-riders under severe weather conditions. The Storm Warning Observatory at Lake Balaton was founded with the aim of providing warnings 1–2 hours earlier for the holiday-makers on the expected wind gusts exceeding 12 or 17 m/s.

In wind forecasting, one of the most difficult tasks is to predict the numerical measures in wind strengthening associated with Cb-clouds as they may be related to different synoptic situations. *Fawbush* and *Miller* (1954)

worked out a simple method for the prediction of maximum wind velocities associated with non-frontal thunderstorms. This method is based on the idea of *Brancato* (1942) that there is a close relationship between the temperature decrease induced by thunderstorms and the maximum wind velocity at the surface.

In the 60's, applicable methods for the prediction of maximum wind velocities with Cb-clouds and squall-lines have already been developed in Hungary, too. These methods originating from the era before the establishment of weather radar observations in our service are well-known after *Bodolainé Jakus* and *Götz* (1963), *Götz* (1963), *Ambrózy* and *Tänczer* (1963), *Bodolai et al.*, (1967). From the beginning of the 70's, identification of Cb-clouds and qualitative estimation of wind gusts associated with Cb-clouds have been completed by radar data. In connection with this, new problems have arisen concerning the very short range ($t \leq 2$ hours) forecast of the wind velocity. In particular, following each radar observation, it has been necessary to estimate to which wind category the maximum wind gusts (V_{max}) connected with Cb-echoes belong from the point of view of the storm warnings: no warning (0), alert (1) or storm warning (2). These wind categories are as follows: category 0: $V_{max} < 12$; category 1: $12 \leq V_{max} \leq 17$; category 2: $V_{max} > 17$ m/s. The objective answer was expected from a decision method. For this reason in the 80's, a decision model was developed (*Bartha*, 1987) to estimate the maximum wind gusts associated with Cb-clouds measured by radar. In the everyday practice of storm warning, this procedure can be executed interactively on a computer (*Bartha* and *Zsikla*, 1990). It combines the method based on conventional data with the approach of using weather radar information. This procedure provides an objective foundation for storm warning services at Lake Balaton.

2. *Decision method for prediction of maximum wind gusts associated with Cumulonimbus clouds*

The developed decision method is based on radar, upper-air and synoptic observational data as well as their combinations. The input parameters and data (*Table 1*) used for the decision procedure can be brought into connection with the maximum wind gusts induced by cold air spreading out at the surface under a Cb-cloud. The summary of the decision system is shown in the block diagram in *Fig. 1*:

— It can be seen that the very short range forecast for the region of Lake Balaton serves as basis for the decision-making on storm warning.

— Whenever precipitation systems detectable by satellite and weather radar appear within the closer area of the lake and their vertical development as well as intensity reach or exceed certain threshoulds ($H_{max} \geq 4$ km; $\lg Z_3 > 0$) more frequent radar observations are initiated. In cases when radar

data do not reach the given threshoulds, the warning changes for conventional decision.

— Then input data contained in Table 1 are fed into the decision system, classifying the Cb-echoes on the basis of wind-hazardous degrees.

— It is followed by consideration of the actual weather situation that may have influence on the development of Cb-clouds. The significant weather objects (denoted by letters C, G, H, I, J, MCC and defined later) are analysed one or three hourly on meso-synoptic charts. The surface pressure patterns

Table 1. Input data used for the objective decision procedure

Radar	Upper-air	Surface
measured parameters		
H_{max}, lgZ_3	H_{trop}, $H_{-20°C}$	T_{akt}, V_{max}, p
reduced parameters		
$Y=H_{max}\,lgZ_3$ $\Delta H=H_{trop}-H_{max}$ $\Delta H^*=H_{max}-H_{-20°C}$	Θ_{wo} Θ_k T_{max}^{prog}	$\Delta T=T_{akt}-\Theta_{wo}$ $\Delta T_{max}=T_{max}^{prog}-\Theta_{wo}$ Δp
Weather characteristics		
Marked weather object	Surface pressure pattern	Bagrovian analogy
codes		indices
C, G, H, I, J, MCC	A, E, F, K, L, M, N, O	$\{\rho_\varphi\}$ ground, 500 hPa $\{\rho_\lambda\}$ ground, 500 hPa $\{\rho_\varphi\,\rho_\lambda\}$ ground, 500 hPa

List of symbols

H_{max} – radar echo top
Z_3 – radar reflectivity factor
H_{trop} – height of tropopause
$H_{-20°C}$ – height of -20°C level
Y – criterion of severity
Θ_{wo} – wet-bulb potential temperature of 0°C level
Θ_k – potential temperature of the Cumulus condensation level
T_{akt} – actual temperature
V_{max} – maximum wind gust observed
p – surface pressure
ΔT – cooling rate
ΔT_{max} – maximum cooling rate
Δp – surface pressure gradient
T_{max}^{prog} – maximum temperature predicted

C – convergence zone
G – warm front
H – instability line
I – cold front
J – occluded front
A – no gradient ($\Delta p < 1$ hPa/100 km)
E – divergence
F – prefrontal gradient situation
K – postfrontal gradient situation
L – Genoa-cyclonic situation
M – Azores anticyclonic situation
N – cyclone over the Carpathian-basin
O – anticyclone over the Carpathian-basin
MCC – meso-scale convective complex

(denoted by letters A, F, L, M, N, O and defined in Table 1) are determined by the hourly change of the horizontal pressure gradient (Δp). The decision-making requires the monitoring of changes in the cooling rate (ΔT) as well as in the maximum wind gusts (V_{max}) measured by a telemetry system around Lake Balaton and in the surface pressure gradient (Δp) in the region of West-Hungary.

— Finally, the decision procedure results in one of the decisions: no warning, alert or storm warning.

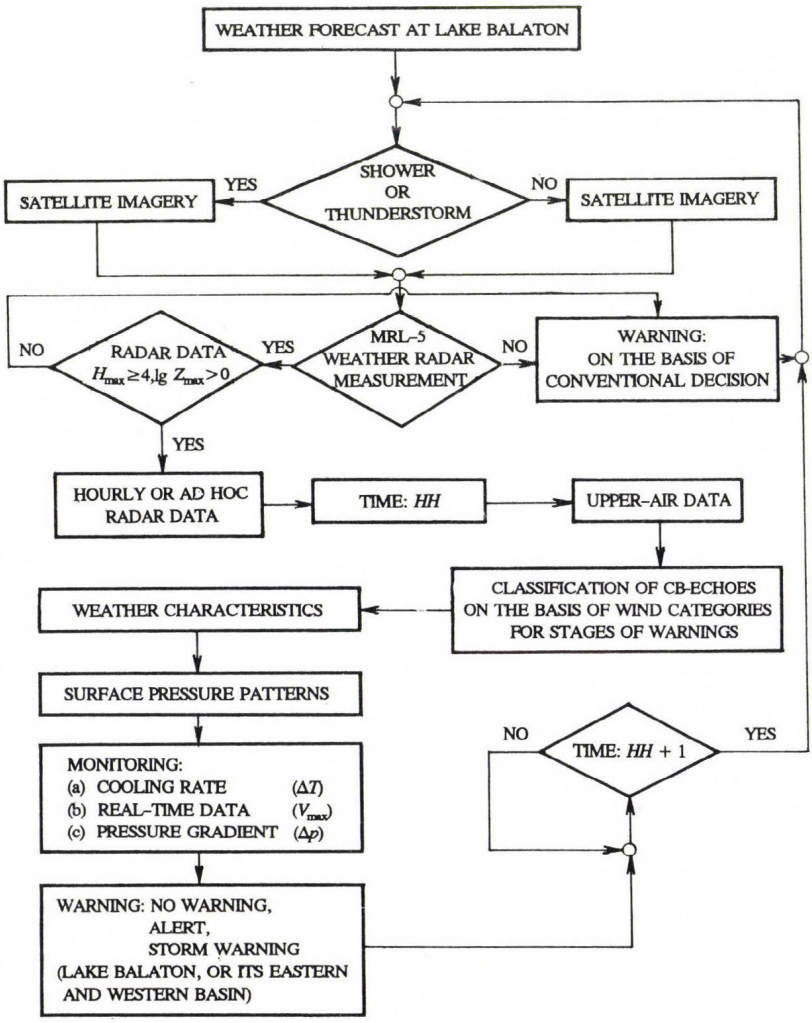

Fig. 1. Block diagram of the objective decision system for forecasting the maximum wind gusts (V_{max}) associated with Cb-echoes.

The programme using the computerized interpretation of manually digitized radar data has been working since 1988. The decision method was tested for the independent decision samples using the observational data of Szentgotthárd/Farkasfa weather radar station in West-Hungary. Warnings issued by the use of computerized decision procedure and those based on conventional method were compared in 548 cases of 1986, 1987, 1989 and the former ones proved to be more reliable by 5% as compared to the conventional ones (the value of accuracy increased from 76% to 81%). At the same time the objective procedure reduced the cases of overestimation by 10% (*Bartha* and *Zsikla*, 1990).

As a development, this decision method used in the storm warning practice also requires the knowledge of permanence for wind-hazards during various weather conditions connected with Cb-clouds (*Bartha et al.*, 1989).

3. Development of decision method

Answers were searched for the following questions from the view-point of wind hazards associated with Cb-clouds:

— Since when has a Cb-cloud become wind-hazardous at the surface?
— Is there difference between the permanence of wind-hazardous degrees associated with Cb-clouds developed during various weather situations?
— How long wind-hazardous periods can be estimated in various weather situations?

3.1 Data used as the starting point for investigation

In order to answer the above-mentioned questions, some active cold fronts (I: cold front or cold front with warm wave) and convective systems (C: convergence zone; H: instability-line; MCC: meso-scale convective complex) were studied. These weather situations (36 frontal and 20 convective storms) were collected in 1986 and 1987 during the periods from May to September. The following data were used for investigation:

— hourly radar observational data (H_{max}; lgZ_3; $Y=H_{max}\ lgZ_3$) from the detection region with a radius of 150 or 200 km of the Szentgotthárd/Farkasfa weather radar station in West-Hungary (the radar is of MRL-5 type and worked on the wavelength of 10 cm, producing information for square elements of 20x20 km^2),
— observational data for the Cb-clouds (SYNOP: $C_L=3$ or 9) and some significant weather phenomena [shower; thunderstorm; hailstorm; wind gusts (V_{max}) associated with Cb-clouds of 7 m/s or stronger] of 13 principal surface synoptic stations in West-Hungary,
— one or three hourly meso-synoptic charts analysing the development and

movement of frontal and convective systems over the region of West-Hungary.

The integration in space and time of radar and surface synoptic observations for the Cb-clouds and their significant weather phenomena was guaranteed by following the considerations of *Brüljov* and *Nizdojminoga* (1977).

The radar and surface observational data connected with Cb-clouds were considered uniform Cb-cloud or significant weather phenomenon in space if one of the principal surface synoptic stations has already observed within a radius of 30 km of maximum reflectivity factor (Z_{3max}) for Cb-echo measured by radar. In consequence of the limited observational area of the principal surface synoptic stations those Cb-clouds and Cb-echoes were considered as simultaneous observational data that were detected by radar within 30 minutes before or after the observation of suitable surface synoptic station(s). In this way, simultaneous data in space and time from the region of West-Hungary were at our disposal in 159 cases.

3.2 Results

It is known that the downdraught within a developed Cb-cloud starts from the height of about 0°C level. The outflowing cold air spreads out at the surface under the Cb-cloud and produces a gust front at its boundary with the ambient air, creating localized, strong, cold winds, squall-lines and large direction changes that are frequently associated with thunderstorms, showers or hailstorms. On that account, the maximum wind gusts connected with Cb-clouds can be expected either simultaneously with the first observation of heavy shower or thunderstorm, or else soon after. As a verification, the frequency distribution of intervals $[\Delta t = t_{V_{max}} - t_{shower;\, thunderstorm}]$ development time ($t_{V_{max}}$) of maximum wind gusts with shower or thunderstorm and the surface observational time $[t_{shower;\, thunderstorm}]$ the same significant phenomena were investigated (*Fig. 2*).

As it follows from Fig. 2, the overwhelming majority (84%) of maximum wind gusts with Cb-clouds developed simultaneously with the first surface observation of heavy shower or thunderstorm and afterwards. The synoptic background of the cases for intervals $\Delta t < 0$ and $\Delta t \geq 2$ hours was also studied. The maximum wind gusts observed with interval $\Delta t < 0$ (in 16% of the cases) were the results of the Cb-clouds with cold front (I) or instability line (H). It is in accordance with the fact that the gust front may propagate in the boundary layer for distance up to 80–100 km away from severe thunderstorm source (*Browning* and *Collier*, 1982). In case of interval $\Delta t \geq 2$ hours, the maximum wind gusts developed in pre- or postfrontal isobaric structures with strong surface pressure gradient (in 9% of the cases) were associated with the Cb-clouds of frontal (I) or convective systems (C or H). On the basis of discussion for Fig. 2, the maximum wind gusts developed either during the first

surface observation for heavy shower and thunderstorm or soon after within 2 hours in 75% of the cases. Consequently it is most likely that the wind-hazardous period of the weaker convective systems developed within the same air mass is equivalent to the interval of $0 \leq \Delta t < 2$ hours.

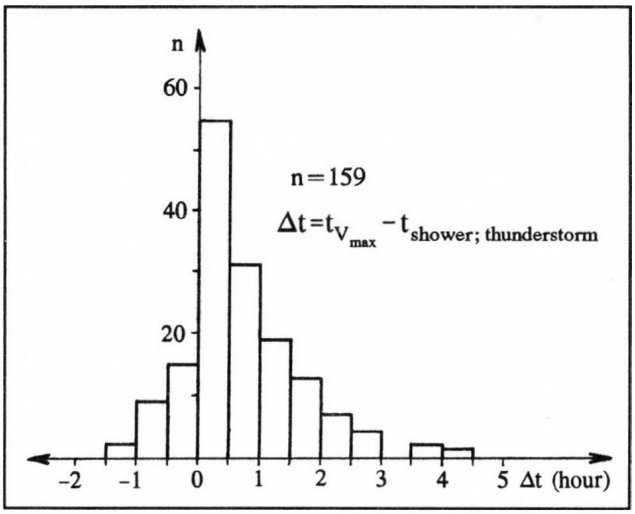

Fig. 2. Frequency distribution of intervals [$\Delta t = t_{V_{max}} - t_{shower;\ thunderstorm}$] between the development time ($t_{V_{max}}$) of maximum wind gusts associated with shower originating from Cb-cloud or thunderstorm and the surface observational time [$t_{shower;\ thunderstorm}$] for the same significant phenomena in case of frontal and convective systems in the region of West-Hungary (1986-1987).

Further investigations were needed to introduce the idea of potential and effective wind-hazardous periods:

— *Potential wind-hazardous period* (Δt_{pot}) is the term when the wind velocity is rapidly and permanently increasing or the gusts are exceeding the value of 7 m/s, associated with Cb-cloud or their significant weather phenomena. These wind gusts develop in the process of downdraught when the outflowing cold air spreads out at the surface under a Cb-cloud.

— *Effective wind-hazardous period* (Δt_{eff}) is the term when the wind velocity is rapidly increasing or the gusts are exceeding the value of 12 m/s, associated with Cb-clouds or their significant weather phenomena. These wind gusts can be expected at the surface whenever the radar detects Cb-echoes with the value of $Y = H_{max} \lg Z_3 \geq 10.9$ (*Bartha*, 1987).

Using these fundamental ideas we investigated the permanence of potential and effective wind-hazardous periods (Δt_{pot} and Δt_{eff}) during different synoptic situations connected with Cb-clouds. The results are shown in *Figs. 3, 4* and *5*. These figures illustrate the empirical probability distribution functions for the

potential and effective hazardous periods of maximum wind gusts associated with frontal (I) and convective systems (C, MCC, H). On the basis of Figs. 3 and 4 it can be seen that the distribution functions for potential and effective

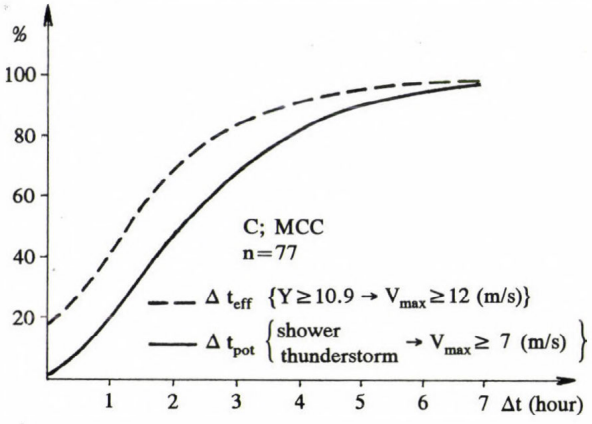

Fig. 3. Empirical probability distribution functions for the potential and effective hazardous periods (Δt_{pot} and Δt_{eff}) of maximum wind gusts (V_{max}) associated with non-frontal thunderstorms in convergence zone (C) or meso-scale convective complex (MCC) in the region of West-Hungary (1986-1987).

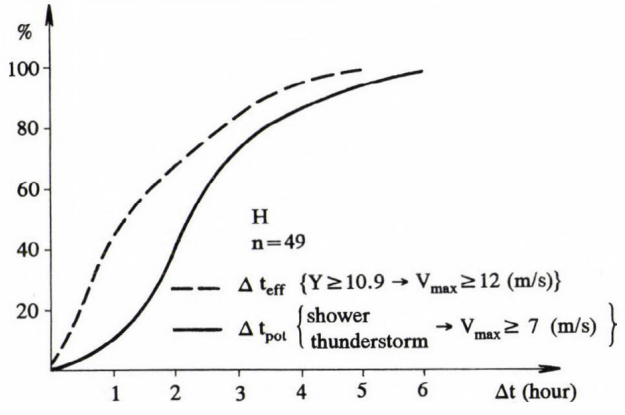

Fig. 4. Empirical probability distribution functions for the potential and effective hazardous periods (Δt_{pot} and Δt_{eff}) of maximum wind gusts (V_{max}) associated with instability lines (H) in the region of West-Hungary (1986-1987).

hazardous periods of maximum wind gusts connected with non-frontal (C, MCC, H) thunderstorms are similar to one another but at the same time they are not similar to the curves for the frontal (I) cases in Fig. 5. Within the convective systems, as it follows from the figures, the empirical probability is nearly zero (2%) when the maximum wind gusts associated with the intensive

radar echoes ($Y \geq 10.9$), belonging to instability lines (H) do not reach the value of 12 m/s. Furthermore, this probability value increases to 17% in case of weaker convective systems (C, MCC).

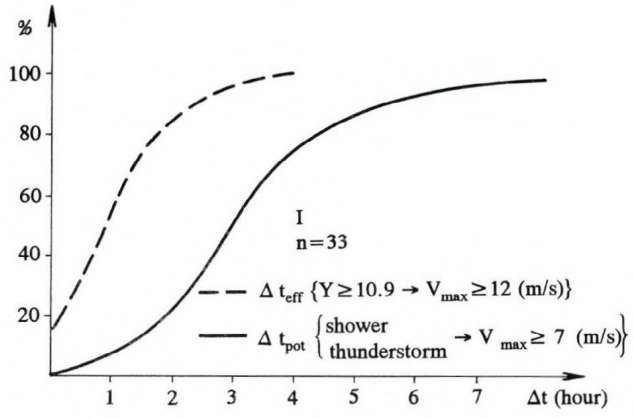

Fig. 5. Empirical probability distribution functions for the potential and effective hazardous periods (Δt_{pot} and Δt_{eff}) of maximum wind gusts (V_{max}) associated with the thunderstorms of cold fronts (I) in the region of West-Hungary (1986-1987).

The results are in accordance with the theoretical and practical results which differentiate between the instability lines and other convective systems from the point of view of wind-hazards (*Götz*, 1965; *Bodolainé Jakus* and *Vissy*, 1990). On the basis of discussions for Figs. 3, 4 and 5, the effective wind-hazardous periods concerning the weaker convective systems (C, MCC) and instability lines (H) proved to be shorter by 0.5–1 hour on the average as compared to the potential ones. Similarly, the same period proved to be shorter by about 2 hours in respect to cold fronts (I). The permanence of potential wind-hazard for the cold fronts (I) with thunderstorms can be increased by the strengthening surface pressure gradient following the fronts. The above-mentioned differences for wind hazards support those theoretical results and practical observations according to which the major part of the instability energy concentrates and gets free in the convective systems (C, MCC, H) developed into line(s) in front of cold fronts (*Horváth* and *Práger*,1985).

4. Conclusions

— Nowadays, additionally to the conventional synoptic data, weather radar and satellite data are also available for the storm forecasters to analyse the weather situation, especially on the meso- and local-scales and to issue warnings as well as to prepare very short range ($t \leq 2$ hours) forecasts. The

success of the so-called NOWCASTING warnings is largely dependent on the integration of non-conventional information into a complex meso-scale analysis (e.g. *Horváth* and *Práger*, 1990) included into the general synoptic framework.

— In case of weaker convective systems developed within the same air mass over West-Hungary, it is most likely that the maximum wind gusts occur either during the first surface observation for heavy shower or thunderstorm, or soon after within 2 hours.
— From the view-point of storm warning the subjective or objective recognition of instability/squall-line must be performed before identifying this weather object by radar, in accordance with the fact that the gust front may propagate in the boundary layer for distance up to 80-100 km away from the thunderstorm source.
— The permanence of wind-hazards associated with Cb-clouds can be increased by the strengthening surface pressure gradient during pre- and postfrontal weather situations.
— The empirical probability distribution functions (Figs. 3, 4 and 5) concerning the permanence of wind-hazard point out the rational periods for practical application. For this reason these results can be used for the further optimization of the nowcasting decision method.

In the near future, one of our tasks is to go on developing this decision method using digitized satellite data (*Horváth et al.*, 1992) as well as digital radar ones.

References

Ambrózy, P. and *Tänczer, T.*, 1963: Prediction of maximum wind velocities connected to thunderstorms (in Hungarian). *Beszámolók 1962*, Orsz. Meteorológiai Szolgálat, Budapest, 84-87.

Bartha, I., 1987: An objective decision procedure for prediction of maximum wind gusts associated with Cumulonimbus clouds. *Időjárás 91*, 330-346.

Bartha, I., Horváth, Á., Kapovits, A. and *Vissy, K.*, 1989: Development of the forecasting methods using radar information for strong and stormy wind associated with convective activity (in Hungarian). *Final Report* on research work, No. 1-3-86-319, sponsored by the Hungarian Academy of Sciences.

Bartha, I. and *Zsikla, Á.*, 1990: Use of radar echoes in storm warning at Lake Balaton (in Hungarian). *Időjárás 94*, 296-307.

Bodolainé Jakus, E. and *Götz, G.*, 1963: Structure and analysis of instability lines (in Hungarian). *OMI Kisebb Kiadványai*, No. 33, Budapest.

Bodolai, I., Bodolainé Jakus, E. and *Böjti, B.*, 1967: Macrosynoptical conditions for the formation of Slovenian squall-lines and some properties of cold fronts with thunderstorm. *Időjárás 71*, 129-143.

Bodolainé Jakus, E. and *Vissy, K.*, 1990: Meso-scale convective systems determined regionally in the Carpathian basin. *Időjárás 94*, 283-295.

Brancato, G.N., 1942: The meteorological behaviour and characteristic of thunderstorms. *U.S. Weather Bureau*, April.

Browning, K.A. and *Collier, C.G.*, 1982: *Nowcasting*. Academic Press, New York, London, 1-42.

Brüljov, G.B. and *Nizdojminoga, G.L.*, 1977: *Use of radar data in synoptic practice* (in Russian). Gidrometeoizdat, Leningrad.

Fawbush, E.J. and *Miller, R.C.*, 1954: A basis for forecasting peak wind gusts in non-frontal thunderstorms. *Bull. Amer. Metorol. Soc. 5*, 1 .

Götz, G., 1963: Prediction of maximum wind velocities connected to non-frontal thunderstorm (in Hungarian). *Beszámolók 1962*, 97-101.

Götz, G. and *Tänczer, T.*, 1965: Wind storms in the region of Lake Balaton in summer half periods (in Hungarian). *Időjárás 69*, 77-86.

Horváth, Á. and *Práger, T.*, 1985: Study of the dynamics and predictability of squall-lines (in Hungarian). *Időjárás 89*, 141-160.

Horváth, Á. and *Práger, T.*, 1990: A meso-β scale objective analysis for meteorological fields (in Hungarian). *Időjárás 94*, 23-38.

Horváth, Á., H.Zsikla, Á. and *Platz, M.*, 1992: Digitized satellite imagery for mesometeorological applications (in Hungarian). *Meteorological Notes of Universities* No. 6, I. 112-123.

IDŐJÁRÁS

Quarterly Journal of the Hungarian Meteorological Service
Vol. 97, No. 2, April–June 1993

Adapted Gaussian plume model characteristics and space-time structure of the estimated SO_2-concentration field due to elevated sources

N. Romanof and **S. Tumanov**

National Institute of Meteorology and Hydrology,
97 Bucureşti-Ploieşti Highway, 71581 Bucharest, Romania

(Manuscript received 8 September 1992; in final form 30 April 1993)

Abstract—The consequences on the air quality of a coal fired power station planned to be located near Turnu Severin, Romania, were assessed using Gaussian plume model estimations along with a significant number of time series of SO_2 hourly concentrations (01, 07, 13 and 19 h) estimated through the same model in the points of a grid around the power station. Beside the "classical" outputs of the model, some upper quantiles and other statistical characteristics of the concentration sets were estimated in each grid-point based on the lognormal and Eggenberger-Polya probability laws.

The time structure of the concentration field has been investigated using a Markov chain for two states: under and over the proper air pollution standard; this allows the calculation of the Besson persistence coefficients which can be useful when air pollution forecasting is attempted.

Correlation coefficients between paired grid-point concentration series were calculated, too, which resulted in areas of representativeness for the main grid-points, defined by equal correlation coefficient (say, 0.75) curves. This can be used in air quality monitoring network planning.

Key-words: Gaussian model, concentration field, Eggenberger-Polya distribution, lognormal distribution, time series model, Markov chain, time-space structure of the field, correlation coefficient, Besson persistence coefficient, area of representativeness.

1. Introduction

As compared to routine air quality studies for planned facilities, this paper was intended to provide more detailed information on the estimated time and spatial characteristics of the concentration field around a point source. The source was a coal fired power station (see the emission characteristics in *Sec-*

tion 3) near Turnu Severin, a medium size town in the south-western part of Romania, on the bank of the Danube. No on-site aerometric measurements were available nor any relief data of the (rather uneven) surroundings were used in the model application, so that the only features characterizing the air flow over the area could be incorporated in the routine meteorological data provided by the near station.

2. *The dispersion model*

The most largely accepted model which is used for the estimation of the air pollutant concentrations due to continuous emission point sources in steady meteorological conditions is the Gaussian plume model (*Hanna*, 1982).

The main problem that arises in applications of the Gaussian model is how to choose the appropriate formulae for the plume rise Δh and dispersion parameters σ_z and σ_y. This choosing must be based upon a preliminary analysis of the experimental data which has generated the relationships for the dispersion parameters and plume rise. For this latter the formulae used in this study were selected on the requirement for the ratio $\Delta h_{\text{observed}}/\Delta h_{\text{calculated}}$ to be as close as possible to the unity. According to *Trampf* (1973), the following expressions seem to be the most suitable and consequently have been selected $\Delta h=(1.5\ WD+9.5\times10^{-6}\ Q_H)/u$ (Holland, for neutral and unstable stratifications), and $\Delta h=(-1.04\ WD+0.6708\ Q_H^{1/2})/u$ (Moses-Carson, for stable stratification); the corresponding $\Delta h_{\text{obs}}/\Delta h_{\text{calc}}$ ratios were 1.00 and 1.05; here D is the stack diameter at the top level (m), W is the exit velocity of the effluent (m s^{-1}), and Q_H is the heat release (W).

There were two stacks in view at Turnu Severin (both are) of 280 m height; this is the reason for which a careful analysis of the dispersion parameters is needed, as these have resulted from various experiments (*IAEA*, 1980; *Briggs* and *Binkowski*, 1985). The relationships for tall stacks were selected and a set of dispersion parameters σ_z and σ_y was derived through statistical treatment as averages over several specific experiments. In the authors' view, such average parameters lead to more realistic estimations than if parameters from single experiments were used.

The dispersion parameters were assumed in the usual form

$$\sigma_z = a\,x^b \quad \text{and} \quad \sigma_y = c\,x^d$$

(x is the downwind source-receptor distance), the coefficients a, b, c and d, and the coefficients of determination r_z and r_y for the exponential curve fit are shown in *Table 1* for each Pasquill stability class. These values were used in the estimations presented in *Section 3*.

Table 1. Coefficients *a, b, c* and *d*, and the coefficients of determination r_z and r_y

Stability class	a	b	r_z	c	d	r_y
A	0.044	1.347	0.999	0.921	0.880	0.999
B	0.136	1.076	0.996	0.530	0.898	0.999
C	0.153	0.960	0.999	0.659	0.827	0.999
D	0.259	0.811	0.999	0.434	0.822	0.999
E	1.124	0.544	0.999	0.685	0.750	0.999
F	0.978	0.516	0.999	0.629	0.769	0.999

2.1 Estimating statistical parameters

Estimation functions for the statistical parameters used herein are presented below; the information content brought about by these is thought to be large enough for decision making.

The relationships for the estimation of the statistical parameters depend upon the way as the concentrations are available throughout the grid. In case when for each meteorological state m (in air pollution studies, m is generally defined by the wind direction D, wind velocity u, and stability class S; but in selected cases, air temperature, mixing height and others are being added) the corresponding concentration $C(x,y,m)$ is known in each grid-point together with the corresponding joint frequencies, then one-point statistical parameters can be estimated in the points (x,y), which characterize the statistical distribution of the concentrations without any space-time statistical correlation between points. In such cases the following estimation functions for the corresponding parameters can be estimated:

Arithmetic mean, $\bar{C}(x,y) = \sum_m C(x,y,m) f(m)$, where m runs the overall set of meteorological states, and $f(m)$ is the frequency of the state m. This frequency can be estimated from a series of meteorological observations (long enough), provided by the meteorological station accepted as representative for the region where the pollutants are dispersed.

Standard deviation, $s(x,y) = \{\sum_m [C(x,y,m) - \bar{C}(x,y)]^2 f(m)\}^{1/2}$.

Cumulative frequency for a given concentration threshold C_p to be exceeded, $G(C_p) = \sum_m f(m)$, *for* $C(m) > C_p$.

Direct use of the Gaussian plume model for the estimation of the expected frequencies for given thresholds C_p to be exceeded is objectionable because uncertainties can occur in the case of extreme weather situations with small frequencies (*Cats*, 1978; *Ludwick et al.*, 1980). This is the reason for which the Gaussian model should be used for its sure estimations, i.e. $\bar{C}$ and s, while for

the cumulative frequencies and quantiles one should resort to selected probability laws, previousely proved to fit frequency distributions of the concentrations. Having this in view, estimations of the expected cumulative frequencies and quantiles based on lognormal and Eggenberger-Polya probability laws are shown below. This latter is more suitable for single sources (*Tumanov*, 1979, 1990).

Statistical distributions used jointly to the Gaussian model.

Beside the main statistical characteristics provided by the Gaussian dispersion model (long term arithmetic mean, mean square deviation and empirical distribution function), some other statistical characteristics were estimated resorting to the two probability laws mentioned above, each of them applicable, as it is known, in specific conditions. The former is the lognormal distribution (*Larsen*, 1971), suitable for urban areas, where there are large numbers of pollution sources spread quite even all over the areas, so that in a given point the concentration does not depend practically on the wind direction. The latter is the Eggenberger-Polya discrete distribution (*Brooks* and *Carruthers*, 1953) which provides right estimations in the case of the concentration series due to single sources (*Tumanov*, 1979, 1990).

Lognormal distribution. The complementary distribution function for the random variable C (the pollutant concentration in a given grid-point), standing for the cumulative probability to equal or exceede a given value c of the concentration C is

$$G(c) = \mathrm{Prob}[C \geq c] = \frac{1}{(2\pi)^{1/2}} \int_c^{\infty} e^{-z^2/2} dz, \tag{1}$$

where $z = \ln(c/m_g)/\ln s_g$, m_g is the geometric mean, and s_g is the geometric deviation of the concentrations, namely (*Larsen*, 1971)

$$s_g = \left[\ln\left(\frac{s}{\overline{C}^2} + 1\right)\right]^{0.5}, \qquad m_g = \frac{\overline{C}}{\exp\left(0.5 \ln^2 s_g\right)}. \tag{2}$$

$\overline{C}$ is the arithmetic mean, and s^2 is the variance of the concentrations.

A C_p-quantile in the case of the lognormal distribution can be expressed as (*Larsen*, 1971)

$$C_p = m_g s_g^{z_p}, \tag{3}$$

where p is the order of the quantile, and the corresponding z_p (see Eq. 1) can be found by solving the equation $G(c)=1-p$.

Different p-order quantiles were calculated up to $p=0.999943$; this latter

corresponds to $p=1-1/17{,}520$, i.e. the cumulative probability of the maximum element out of 17,520 values covering a one year time period of 30-minute average concentrations: this probability has been chosen according to the way as the air quality standards are usually set. The same quantiles were calculated for the Eggenberger-Polya distribution (see below).

It is reminded that a p-order quantile C_p is that value of the distribution for which there is the probability p for the concentration to be less than C_p; that is in $p \cdot 100$ per cent of the time the concentration is expected to be less than C_p in a given point, or, further, C_p is that concentration which will be equalled or exceeded with a probability $1-p$, or in $(1-p)\cdot 100$ per cent of the time. If, for instance, $C_{0.999943} \geq C_{\text{max.permissible}}$ it follows that the air quality standard is violated.

Eggenberger-Polya distribution. The cumulative probability $F(c)$ is given by the expression

$$F(c) = \text{Prob}[C>c] = \sum_{k=0}^{c} p_k . \tag{4}$$

p_k are the Eggenberger-Polya discrete probabilities (*Brooks* and *Carruthers*, 1953):

$$p_0 = \frac{1}{(1+d)^{\bar{C}/d}}$$

$$p_k = \frac{\bar{C}(\bar{C}+d)(\bar{C}+2d)\ \ldots\ (\bar{C}+[k-1]d)}{k!\,(1+d)^{\bar{C}/d+k}} \tag{5}$$

$$k = 1, 2, \ldots$$

where $d = s^2/\bar{C} - 1$.

The complementary distribution function is $G(c)=\text{Prob}[C\geq c]=1-F(c-1)$. Since the Eggenberger-Polya distribution is a discrete one, C is an integer quantity, and it is required for the threshold c to be an integer, too, preferably expressed in $\mu g\ m^{-3}$.

The C_p-quantiles of the distribution are calculated by linear interpolation, in c and p coordinates, between two successive values of the random variable: the first is the greatest integer for which $F(c)\leq p$, and the second is the previous value plus one.

Estimations for the time series case. In case the concentrations in a grid-point are available as time series (one concentration for each observation time), the following relationships are used to calculate the average and variance:

$$\bar{C} = \frac{1}{n}\sum_{i=1}^{n} C_i , \qquad s = \left[\frac{1}{n}\sum_{i=1}^{n}(C_i - \bar{C})^2\right]^{1/2} . \tag{6}$$

One can estimate the empirical distribution function simply by counting the concentrations less than a given threshold and running this latter within the range of the variable.

Time series available in each grid-point can be used to investigate the statistical space and time structure of the concentration field.

2.2. *Time structure investigation based upon a Markov chain model*

A Markov chain model with two states was used: $C \leq 0.75$ mg m^{-3} (the air quality standard for the 30-min SO_2-concentration)–state 1, and $C > 0.75$ mg m^{-3}–state 2. Sequences of random numbers of the form

121122112221211211...

were derived each grid-point. The Markov chain model applied to such sequence allows to find out the type of the statistical (Markov) dependence, i.e. the order of the chain, as well as to estimate the persistence of a given state (for instance, one can estimate the probability to have n times successively the state 2). Such an analysis was first made for SO_2 daily mean concentrations measured at Copşa Mică (*Romanof*, 1982).

We now define a set of statistical quantities and estimation functions for the Markov chains.

Let $p(i)$, $p(i,j)$, $p(i,j,k)$, etc. be the probabilities having the state i, the sequence ij, the sequence ijk, etc. respectively; the indicies ijk assume values 1 and 2. For example, $p(2,2)$ is the probability for the concentration to exceed two times successively the air quality standard.

The statistical dependence is expressed through the so called conditional probabilities: p_{ij} is the probability for the state j provided that at the previous observation time the state i occurred; p_{ijk} is the probability for the state k provided that at the previous observation times the states i and j occurred. If there are four observations a day, p_{22}, for instance, is the probability to exceed the air quality standard at the time h provided that the standard was exceeded at the time h-6.

Denote by $n(i)$, $n(i,j)$, $n(i,j,k)$, etc. the numbers of cases when the states i, ij, ijk, etc. occurred. The probabilities for sequences of states to occur are given by

$$p(i) = \frac{n(i)}{n},$$

$$p(i,j) = \frac{n(i,j)}{n}, \qquad (7)$$

.....

and the conditional probabilities are given by

$$p_{ij} = \frac{n(i,j)}{n(i)},$$

$$p_{ijk} = \frac{n(i,j,k)}{n(i,j)}, \qquad (8)$$

.....

where n is the total number of observations.

The sequence is said to be sequence of independent variables if $p_{...ijk}=p_k$; first order Markov chain if $p_{...ijk}=p_{jk}$; second order Markov chain if $p_{...ijk}=p_{ijk}$, etc. The order of the Markov chain indicates the number of previous states which influences the state at a given moment. Chi-square test can be used as a method to assess the order of a Markov chain (*Mihoc* and *Craiu*, 1972), and this was used herein at a 5% significance level.

The Besson coefficient can be used as a measure of the persistence (*Brooks* and *Carruthers*, 1953):

$$r_B^i = 1 - \left(\frac{1 - p_{ii}}{1 - p_i}\right)^2. \qquad (9)$$

If there is persistence, p_{ii} is greater than p_i. $r_B^i=0$ indicates the absence of the persistence, while $r_B^i=1$ indicates maximum persistence; in certain cases, if p_{ii} is less than p_i, the Besson coefficient can also take negative values, which indicates a tendency for occurrances and non-occurrances to oscillate.

2.3. Spatial structure of the concentration field

The spatial structure was investigated using the coefficient of linear correlation between concentrations estimated in pairs of grid-points:

$$R(x_1,y_1;x_2,y_2) = \frac{\overline{\left[C(x_1,y_1) - \bar{C}_1\right]^2 \left[C(x_2,y_2) - \bar{C}_2\right]^2}}{s_1 s_2}, \qquad (10)$$

where (x_1,y_1) and (x_2,y_2) are the coordinates of the points; $\bar{C}_1$ and $\bar{C}_2$ are the mean concentrations; s_1 and s_2 are the variances. This coefficient is a measure of the degree of statistical dependence between two points, and offers useful information to select measuring points in air pollution monitoring network planning. A line of equal correlation coefficient (e.g. 0.75) around a given

point, say a maximum of a spatial concentration distribution, delimits what could be said to be the area of representativeness of the given point. Dividing a zone of interest into areas of equal correlation is a way to choose measuring points of a monitoring network.

The statistical parameters presented in this section have been estimated and discussed on the base of spatial distribution in *Section 3.*

3. *Results and comments concerning the estimated SO_2-concentration field*

Some input and auxiliary data together with a set of specifications thought to be needed in the discussion are summarized in the beginning of this section.

3.1. Data

Emission data. There were two stacks of 280 m height designed for the power plant; diameter at the top: 8.1 m; exit temperature: 146°C. The emission regime does not depend on the ambient air temperature t_a (emission rate Q=6,193 g s^{-1} SO_2; exit velocity W: 11.53 m s^{-1}), except one of the stacks, for which Q=9,275 g s^{-1}, and W=17.9 m s^{-1} when $t_a \leq 8$°C. It should be mentioned that a set of initially designed emission data are used here, which latter changed but, of course, this fact does not make the procedure proposed less applicable.

The Gaussian model. It was applied in two versions for estimating the statistical parameters of the concentration field: time series version, and frequency based version.

In the time series version, short term (1/2 h) concentrations were generated using 10-year meteorological observations (1971–1980), every 6 hours, provided by the Turnu Severin station: wind velocity and direction, atmospheric stability class, air pressure and temperature. Using these as primary data, 24 h average concentration series were calculated, which allowed Markov type statistical dependence to be studied. As in the primary data the wind direction was reported in sixteen 22.5°-wind sectors, a random direction within each sector was generated based upon the acceptance that all directions are equally probable. In calm conditions, a direction comprised between 0° and 360° was randomly generated, asigning a wind velocity of 1 m s^{-1} to each direction. The Uhlig scheme (*Uhlig*, 1965) was applied to determine the atmospheric stability class.

For the wind velocity vertical profile, a power type law was used for rural areas (*Hanna*, 1982):

$$u(z) = u(10)(z/10)^p \qquad \text{for } z \leq 200 \text{ m};$$
$$u(z) = u(200) \qquad \text{for } z > 200 \text{ m}.$$

$u(10)$ is the wind velocity at 10 m height, and p is an exponent which takes the following values depending upon Pasquill stability classes: 0.07 (A and B), 0.10 (C), 0.15 (D), 0.35 (E), and 0.55 (F/G).

In the frequency based version of the Gaussian model, joint frequencies of the wind direction (2°-wind sectors), wind velocity class (1 m s^{-1} step), and Uhlig stability class (7 classes) were estimated taking into account the slight dependence of some emission characteristics to the ambient air temperature. To preclude underestimations due to calm situations missing from the computations, which is required by the model, the calm case frequencies in the seven stability classes have been asigned to the wind directions proportionally to the first velocity class frequency in each velocity-direction joint frequency matrix.

Computation grid. The grid size was 20 km in the E–W direction by 30 km in the N–S direction; the grid points were 1 km-spaced in the frequency based Gaussian model version (600 grid-points in all); in the time series version, spacing was 1 km in the portions with strong gradients of the estimated fields, and 3 km in the portions away from these (350 grid-points in all).

Computation time. This was 2 min. per grid-point for the frequency based model, and 15 min. per grid-point for the time series based model (FELIX C 512 computer).

3.2. Results: presentation and discussion

Spatial distributions of the statistical parameters estimated using the described procedures are shown in *Figs. 1* to *9* as isolines.

SO_2 annual mean concentrations estimated from ground level wind data can be seen in *Fig.* 1. Three spatial maxima are to be noticed; situated to the NW and SW directions from the source point (marked by dark circle located near Halînga) with concentrations reaching 60 $\mu g\ m^{-3}$, as well as to the E with a maximum of 100 $\mu g\ m^{-3}$ (the 30-min air quality standard for SO_2) are shown in *Fig. 2.*

The frequencies to exceed the 750 $\mu g\ m^{-3}$ threshold, calculated from the Eggenberger-Polya distribution using the estimated long term annual averages and standard deviations (*Tumanov*, 1990) are shown in *Fig. 3.* Although it is known that the lognormal distribution is not suitable for the case of single sources, frequencies were calculated with this distribution, too, as illustrated in *Fig. 4.*

The 0.999943-quantile estimated from the Eggenberger-Polya law (the values on the lines are expected to occur once a year) can be found in *Fig. 5.*

The conditional probability to exceed 750 $\mu g\ m^{-3}$ threshold at the time h if an exceedance occurred at the time h-6 (observations every 6 hours) is presented in *Fig. 6.* The range is seen to be 1 to 10 per cent, indicating a weak statistical time connection in the series. The same effect is shown by the Besson persistence coefficient in *Fig. 7.* Markov chain order can be seen in *Fig. 8,* in

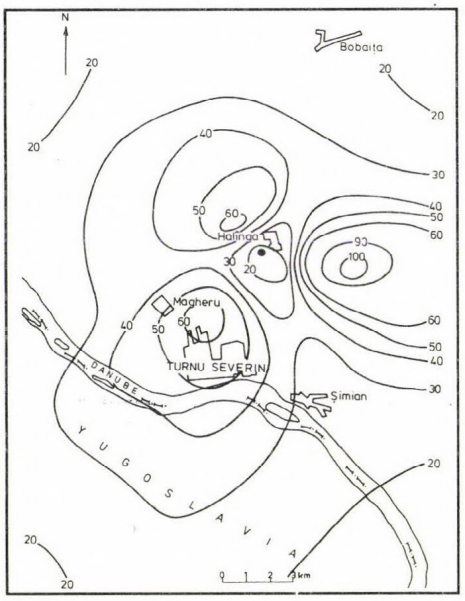

Fig. 1. Annual mean concentration, $\mu g\ m^{-3}$

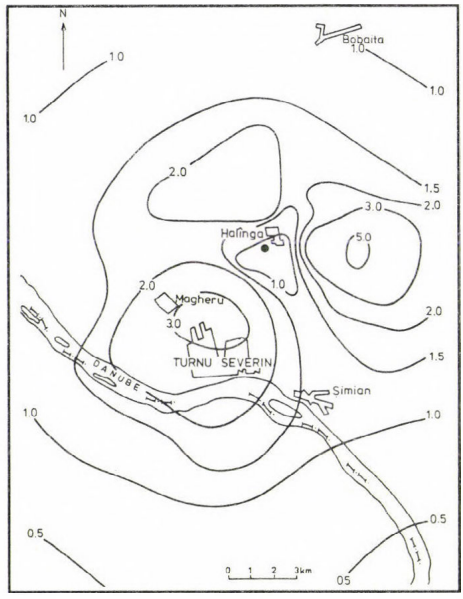

Fig. 2. Frequency to equal or exceed the 750 $\mu g\ m^{-3}$ threshold of the 0.5-h mean concentration, calculated through the Gaussian model.

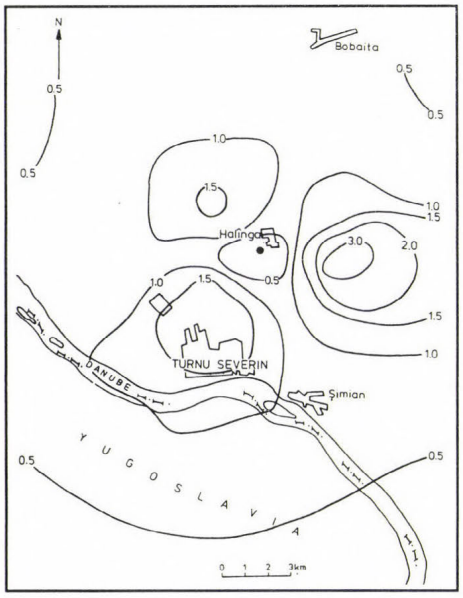

Fig. 3. Frequency to equal or exceed the 750 $\mu g\ m^{-3}$ threshold of the 0.5-h mean concentration, calculated with the Eggenberger-Polya distribution.

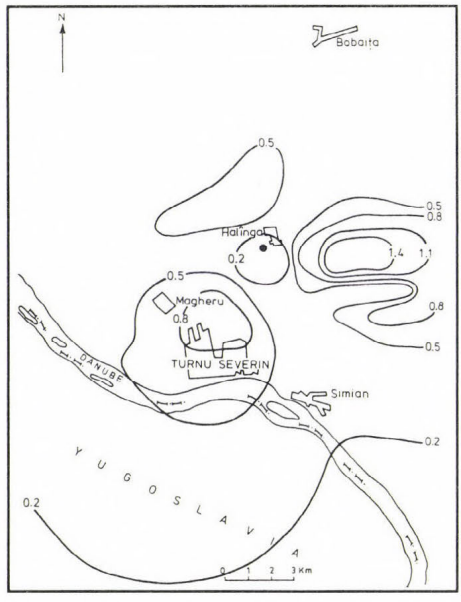

Fig. 4. Frequency to equal or exceed the 750 $\mu g\ m^{-3}$ threshold of the 0.5-h mean concentration, calculated with the lognormal distribution.

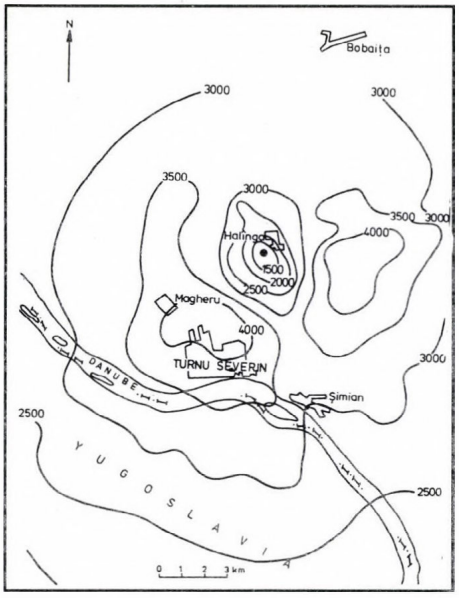

Fig. 5. 0.999943-quantile ($\mu g\ m^{-3}$) calculated from the Eggenberg-Polya distribution.

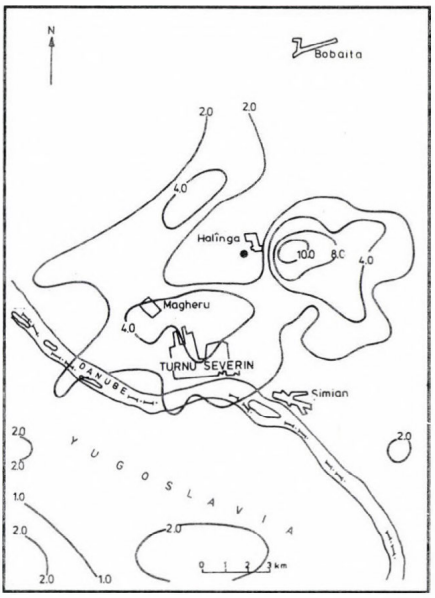

Fig. 6. Conditional probability p_{22}, per cent.

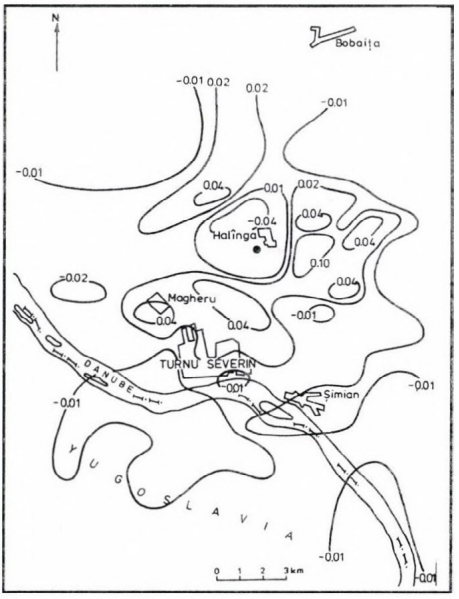

Fig. 7. Besson persitence coefficient r_B^2.

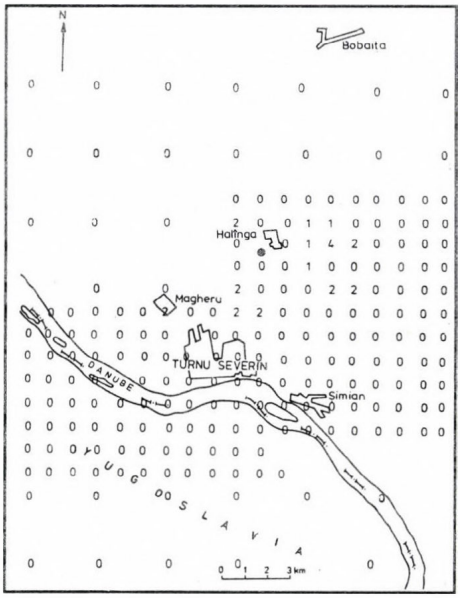

Fig. 8. Markov chain order.

which 0 means that the 6-h spaced concentrations are independent, whereas 1 indicates first order Markov chain, etc. Sparcely, statistical dependence as first to fourth order Markov chains occur in the centres of the maximum mean concentration areas. One could conclude that stochastic methods would hardly be successful in similar cases.

Curves of equal correlation coefficient (0.75) between maximum (M) and neighbouring points are presented in *Fig. 9.* Areas enclosed by such isolines, said areas of representativeness (see *Section 2.3*), could be used to place monitoring points inside them and thereby be sure that in a given grid the number of points would be reduced inside the areas of representativeness. But on the other hand, the areas of representativeness in this case are rather small, and a quite dense monitoring network is required to get reliable data.

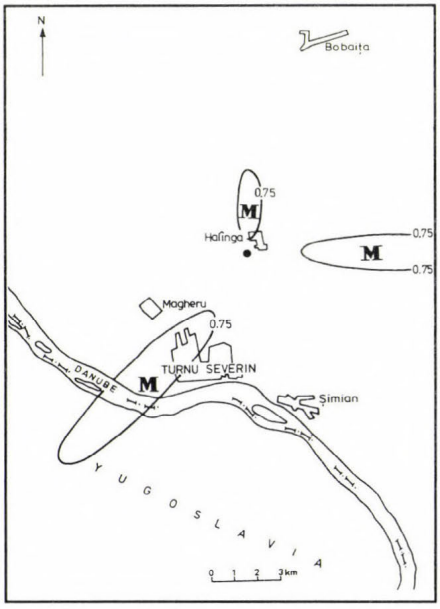

Fig. 9. Areas of representativeness (M) for three monitoring points corresponding to the 0.75 correlation coefficient.

Acknowledgements—The authors would like to thank *Mr. Ion Sandu* for running the computation programme of the Gaussian model. We are particularly grateful to our former colleague *István Elekes* for his valuable programming work aimed at estimating such a great deal of new and "unusual" statistical characteristics of the air pollutant concentration fields.

References

Briggs, G.A. and *Binkowski, F.S.*, 1985: *Research on Diffusion in Atmospheric Boundary Layers: A Position Paper on Status and Needs*. EPA Publication No. 600/3-85/072.

Brooks, C.E.P. and *Carruthers, N.*,1953: *Handbook of Statistical Methods in Meteorology*. Her Majesty's Stationary Office, London, 315-318.

Cats, G.J., 1978: A simple method for quick estimates of frequency distributions of air pollution concentrations from long-term average concentrations. *Proc. WMO Symp. on Boundary Layer Phys. Applied to Specific Problems of Air Pollution*, 19-23 June, Norrköping, WMO No. 510, 157-162.

Hanna, S.R., 1982: Review of atmospheric diffusion models for regulatory applications. *WMO Technical Note* No. 177.

IAEA, 1980: *Atmospheric Dispersion in Nuclear Power Plant Siting*. A Safety Guide, Vienna.

Larsen, R.I., 1971: *A Mathematical Model for Relating Air Quality Measurements to Air Quality Standards*. Env. Prot. Agency, Triangle Park, N. Carolina, Publication No. AP-89.

Ludwick, J.D., Weber, D.B., Olsen, K.B. and *Garcia, S.R.*, 1980: Air quality measurements in the coal fired power plant environment of Colstrip, Montana. *Atmos. Environ. 14*, 523-532.

Mihoc, G. and *Craiu, M.*, 1972: *Statistical Inference for Dependent Variables*. Ed.: Academiei Române (in Romanian).

Romanof, N., 1982: A Markov chain model for the mean daily SO_2 concentrations. *Atmos. Environ. 16*, 1895-1897.

Trampf, W., 1973: *Formeln zur Berechnung der Schornsteinüberhöhung. Speziell für grossemittenten und für kalte Quellen*. Institut für theoretische Meteorologie der Freien Universität Berlin.

Tumanov, S., 1979: Frequency distributions of gas pollutant concentrations measured in the neighbourhood of a high single source. *Meteorology and Hydrology 2*, 11-16.

Tumanov, S., 1990: Statistics of concentrations due to single air pollution sources to be applied in numerical modelling of pollutant dispersion. *Atmos. Environ. 24A*, 1029-1035.

Uhlig, S., 1965: *Bestimmung der Stabilitätsgrade der Luft an Hand von Wettermeldungen*. Mitt. des Deutsches Wetterdienst, Offenbach.

IDŐJÁRÁS

Quarterly Journal of the Hungarian Meteorological Service
Vol. 97, No. 2, April–June 1993

The effects of winter temperature on the migration of insects

A. Stollár*, Z. Dunkel[1], F. Kozár and Diaa A.F. Sheble****

** Hungarian Meteorological Service,*
P.O. Box 38, H-1525 Budapest, Hungary
*** Plant Protection Institute, Hungarian Academy of Sciences,*
Hermann Ottó út 15, H-1022 Budapest, Hungary

(Manuscript received 5 June 1992; in final form 17 May 1993)

Abstract—On the basis of climatological studies it is generally accepted that the increase of the amount of greenhouse gases in the atmosphere can lead to a global warming. However, the degree and impact of warming are not entirely clear. In this paper we study the possible effects of changing climatic conditions on the migration of insect pests. The results of our studies show that during the period of 1881–1990 when the winter temperature increased significantly in Hungary a northward migration of some termophilous pest insects was observed. The decreasing number of short cold periods during the milder winters in the last decades could not stop this northward movement of the insects.

Key-words: migration of insects, winter temperature, changing climatic conditions, regional warming.

1. Introduction

Different living organisms like insect pests require special climatic conditions which are essential for their survival, spreading and migration. Generally, the expansion of the living-environment is possible in two ways. First, during the evolution such species develop which are resistant to a given climate. On the other hand, living-species can migrate to other regions where climate is favourable for their existence. If new species appear in a certain region, both possibilities should be studied to clarify more exactly whether the climatic or the biological factors are more significant for this phenomenon.

As a matter of fact, some new insect pests have appeared in Hungary during this century. Our study focuses on the variation of the winter temperature

[1] Corresponding author address: Z. Dunkel, Institute for Atmospheric Physics, P.O. Box 39, H-1675 Budapest, Hungary.

during the last 110 years which has had considerable impact on the above mentioned process. Due to human activity, the concentration of CO_2 and some other greenhouse gases has increased significantly during the last decades (*Mészáros* and *Götz*, 1988; *Götz*, 1988, 1990; *Mika*, 1987, 1988; *Faragó et al.* 1991). The increasing amount of these gases can lead to global warming, which will affect the climate of Hungary, too. According to studies the warming may reach 1.5–4.0°C by the middle of the next century, however, the exact rate and its regional climatic effects are uncertain. Subsequently, the biological and other consequences of the anticipated climate change can not be clearly determined.

The problems related to new insect pests in Hungary were analysed earlier by *Kozár* and *Dávid* (1986), *Kozár* and *Stollár* (1990) and *Kozár* (1991a, 1991b). The varying climatic conditions have significant implications for other groups of living organisms, as well. *Németh* (1990) and *Solymosi* (1992) have analysed the effect of the climate-variations during this century on some Mediterranean weed species appearing around Eger. In this paper the relationship between the variability of the winter temperature and the spatial distribution of new pests in Hungary is analysed. More concretely, the migration and regional distribution of the *Mediterranean Pseudaulacaspis Pentagona* is studied. This species first appeared around Pécs in 1923 then slowly spread northward, and in 1929 it was already found all over the county Baranya and in some parts of Somogy and Zala (*Fig. 1*). After this initial phase the migration stopped for a long period. In 1976 this pest was found in the southern part of the Hungarian Great Plain moreover in the surroundings of Budapest, too. The migration continued and this species was already found in several places of the county Pest in 1983 and, shortly after in other parts of the country. Similar expansion has been observed for other insects. For example, the *Corytuca ciliata* has spread all over the country in only 15 years (*Fig. 2*). The aim of this study is to find an explanation for the rapid northward movement of different insects.

2. Data and methods

In this study, we used the long-term representative temperature observations from nine stations of the Hungarian Meteorological Service. These continuous observations and the derived data series started in 1881. Thus, we can make our analyses of data on the basis of 110 years of meteorological observations. The location and spatial distribution of these stations are suitable for the determination of the regional differences in the climatic characteristics of our country.

The winter temperature is a determinative factor in the life cycles of the insects, because their resistance is very low in the cold periods with critical temperature minima. Therefore the insects hardly survive the intensive cooling

of the winter. For this reason, the winter (December-January-February) mean temperature was selected as the principal meteorological factor.

In the first phase of our work, we analysed the winter temperatures. We calculated annually the mean temperature of winters from 1881 to 1990 years. After this we calculated the average temperature for the decades 1881–1890, 1891–1900, ..., 1981–1990 for each station, then we represented the draft country-wide regional distribution of this parameter in Hungary. The temperature data were also graphically represented and analysed for the existence of long-term tendencies by linear trend analyses. The spatial distribution and temporal migration of the insects were taken from the surveys made by the Plant Protection Institute, Budapest.

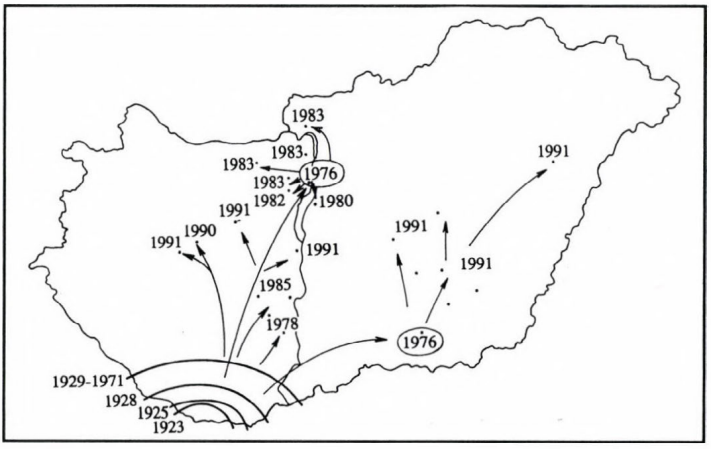

Fig. 1. Migration of *Pseudaulacaspis pentagona* in Hungary.

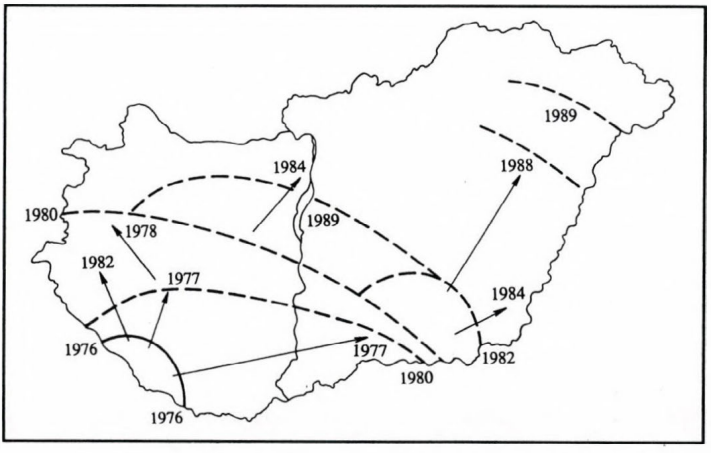

Fig. 2. Migration of *Corytuca ciliata* in Hungary.

3. Results

As it is well known, one of the most important limiting factors in the insect migration is the occasionally low or critical winter temperature. Cold winters decrease the density of the insects because of the high mortality, and in this case the migration will be very slow, or it will stop. After extreme winter situations some insect species can totally disappear from certain regions. On the contrary, the mild winters can result in a rapid increase in the local density of the insects and subsequently an intense migration and extensive distribution of the insects can start to other and new regions.

Analysing the winter temperature for the last 110 years for different parts of the country, considerable fluctuations were revealed everywhere. The maximum amplitude range reaches 8–9°C. The interannual fluctuations are also large in time scale. Very cold winters appeared after mild winters in the last decades. Now there is a question: how did our climate change during last century and there is another question: are 110 years enough to verify it? The trend analysis of winter temperature data shows a slow increase in this parameter for most stations. Analysing the data from 9 stations, we found that this increase of warming tendency was the highest for Budapest (0.016°C per year that can be partly mainly explained by the increasing heat-island effect of the capital. The increase was true also for the coldest eastern regions for instance, around Nyiregyháza the increase was also very high (0.014°C per year). In the southern regions, the estimated increase was not statistically significant much lower, for example in Pécs only 0.005°C per year. The mean trend calculated from the data of the 9 stations, shows an average increase

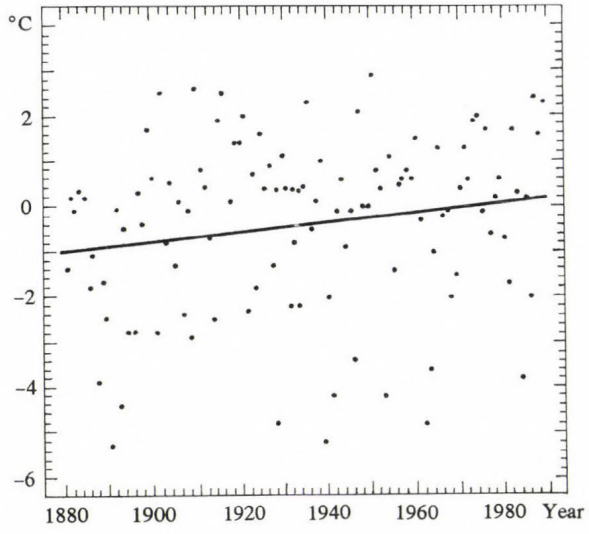

Fig. 3. The averages and trend of winter temperature in Hungary from 1881.

0.011°C per year (*Fig. 3*), and the correlation coefficient of the linear regression is significant at $P=5\%$ level.

In this study we calculated the averages of winter temperature for every decade (*Table 1*). It is also obvious from the above analysis that after the very cold decades at the end of the last century, a slow warming appeared which was followed by a smaller variation of temperature for a long period. The decade of 1961–1970 was again cold, which was followed by warmer periods during the last two decades. The average winter temperature in Hungary, based on the data of nine stations for 110 years was –0.40°C. The regional distribution of winter averages for ten years is shown in *Fig. 4*. The darker places were colder and the lighter were warmer places and periods. The various hatching of the maps shows the fluctuation of winter average temperatures. In Hungary, the decade 1901–1910 was the first one when the winter average above 0°C appeared over the territories of the country and in the next decade this average value continued to increase. It is possible that several termophilous insect species appeared in this period in Hungary, such as the *Pseudaulacaspis Pentagona* also and they could spread to some other regions under warm conditions. The mild winters in area of Pécs and Budapest with an average above 0°C lasted for a long time, could stimulate the survival of the above-mentioned insect species after their first appearance (in 1923). For several decades, these species have occurred only in the southern counties, but after the cold decade of 1961–1970, those appeared in other regions, e.g., in the southern part of the Great Plain and in Budapest where it was found that they appeared in 1976. After 1980 this species continued its spreading into the counties Pest, Komárom, Nógrád and this process continues nowadays. If the mild winters will recur in the future, this species or these species can occupy additional regions of the country.

Table 1. Winter temperature averages (°C) for ten years in different parts of Hungary

Stations	1881-1890	1891-1900	1901-1910	1911-1920	1921-1930	1931-1940	1941-1950	1951-1960	1961-1970	1971-1980	1981-1990	Mean 1881-1991
Pécs	-0.77	-0.27	0.64	1.37	0.36	0.65	0.06	0.71	-0.90	1.06	0.51	0.29
Budapest	-0.69	-0.45	0.68	1.43	0.34	0.01	0.48	0.85	-0.05	2.06	1.26	0.53
Keszthely	-1.21	-0.60	0.44	0.94	-0.20	-0.44	0.15	0.49	-0.18	0.89	0.39	0.05
Szombathely	-1.77	-1.21	-0.22	0.22	-1.02	-1.55	-0.58	-0.60	-1.73	0.60	-0.21	-0.74
Mosonmagyaróvár	-1.53	-1.08	0.09	0.51	-0.64	-0.93	-0.53	-0.17	-1.28	0.83	0.05	-0.45
Kalocsa	-1.40	-0.90	0.07	0.94	-0.28	-0.67	-0.03	0.62	-0.95	0.76	0.33	-0.14
Szeged	-1.73	-1.27	-0.15	0.65	-0.26	-0.99	-0.22	0.14	-1.23	0.71	0.07	-0.40
Debrecen	-2.14	-1.91	-0.78	-0.02	-1.07	-1.69	-1.12	-0.48	-1.83	-0.13	-0.75	-1.10
Nyíregyháza	-2.69	-2.40	-1.67	-0.85	-1.69	-2.11	-1.01	-1.04	-2.30	-0.45	-1.13	-1.63
Country mean	-1.52	-1.21	-0.10	0.58	-0.50	-0.86	-0.41	0.06	-1.16	0.70	0.06	-0.40

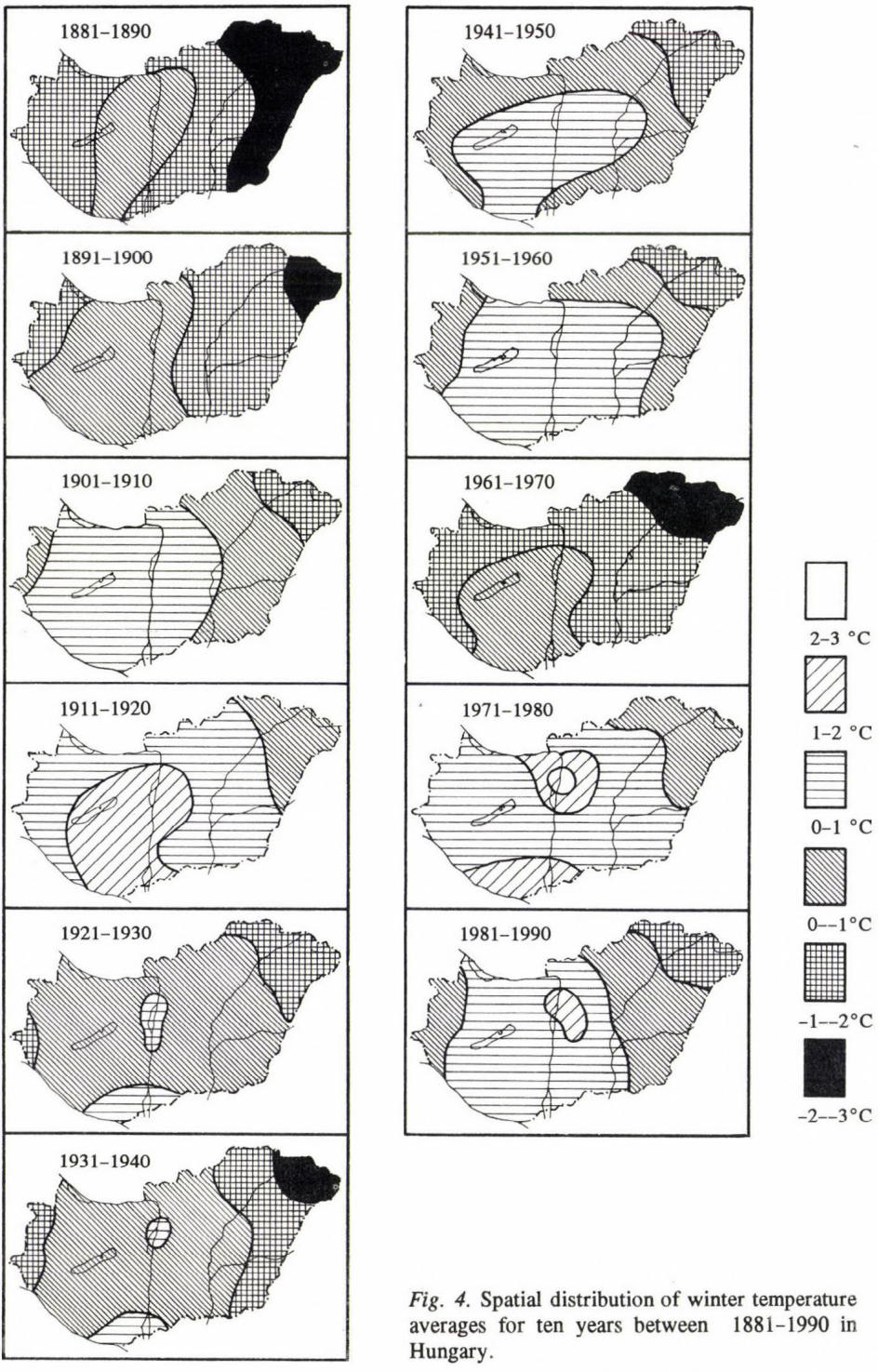

Fig. 4. Spatial distribution of winter temperature averages for ten years between 1881–1990 in Hungary.

4. Conclusions

Analysing the averages of winter in Hungary from the beginning of the systematic meteorological observations (1881), we found a great fluctuation in the annual data. Using the temperature averages of decades instead of the annual average, we can see cold decades in 1931–1940 and 1961–1970 followed the previous warmer periods. The linear trends of the winter averages for different stations show a slow increase. The country-wide average of winter temperature indicates a significant increase of 0.01 °C per year and it means an 1 °C increase per 100 years. The changing temperature will affect animal and plant communities. New species appear, which could alter the species composition. The new pest and weed species can cause serious problems in agriculture.

The higher averages of the winter temperature in the southern and middle parts of Hungary and surroundings of Budapest compared with the migration process of insects in time show good correlation. In the future the study of the appearance, migration and distribution of termophilous insect and weed species require more attention. The winter mortality data would help to clarify the impact of an expected global warming on the life of insects.

References

Faragó, T., Iványi, Zs. and *Szalai, S.*, 1991: *Climate variability and change II.* OMSZ, Budapest, 1-218.

Götz, G., 1988: Climatic variations and predictability (in Hungarian). *Időjárás 92*, 140-152.

Götz, G., 1990: Century of the effect of greenhouse gases (in Hungarian). *Tudomány 6*, No. 9, 16-22.

Kozár, F., 1991a: Global warming and the living nature in Hungary (in Hungarian). *Természet Világa 122*, 515-517.

Kozár, F., 1991b: Recent changes in the distribution of insects and the global warming. *Proceedings of European Congress of Etymology*. Budapest, 1-10 (in print).

Kozár, F. and *Dávid, A.*, 1986: The unexpected northward migration of some species of insects in Central Europe and climatic changes. *Anz. Schadlinskunde, Pflanzenschutz und Umweltschutz 59*, 90-94.

Kozár, F. and *Stollár, A.*, 1990: Do the insects predict climate change (in Hungarian)? *Élet és Tudomány 30*, 939-940.

Mészáros, E. and *Götz, G.*, 1988: The future of our climate (in Hungarian). *Magyar Tudomány 95*, 562-570.

Mika, J., 1987: Application of the annual cycle of meteorological elements to estimate the regional properties of global climate change (in Hungarian). *Időjárás 91*, 34-42.

Mika, J., 1988: Regional features of a global warming in the Carpathian Basin (in Hungarian). *Időjárás 92*, 178-180.

Németh, I., 1990: Appearence of Mediterranean weed species in the region of Eger (in Hungarian) (ed.: I. Seprős). Növény-

védelmi Tudományos Napok 1990. Összefoglalók. Budapest, 127.

Solymosi, P., 1992: Indigeneous and adventive vegetation in Hungary (in Hungarian). *Növényvédelem 28*, 1-15.

IDŐJÁRÁS

Quarterly Journal of the Hungarian Meteorological Service
Vol. 97, No. 2, April–June 1993

The flying activity of turnip moth (Scotia segetum Schiff.) in different Hess-Brezowsky's macrosynoptic situations

L. Nowinszky*, Cs. Károssy* and Gy. Tóth**

* *Teacher's Training College "Berzsenyi Dániel", P.O. Box 170, H-9701 Szombathely, Hungary*
** *Gothard Astrophysical Observatory of Roland Eötvös University, H-9707 Szombathely, Hungary*

(Manuscript received 15 October 1992; in final form 8 June 1993)

Abstract—The collection of insects by light-trap is a wide-spread sampling method of plant-protection, but its efficency is influenced by many environmental factors especially the weather. Knowing these influencing parameters, one can elaborate more reliable prognoses.

The authors pointed out in their earlier paper that the macrosynoptic weather types of *Péczely* are very useful for investigation of insect ecology in territory of Carpathian-Basin.

The present paper deals with macrosynoptic situations of *Hess-Brezowsky* extended for the whole Europe in connection with the flying activity of a harmful insect, the turnip moth (Scotia segetum Schiff.) being represented by the number of collected individuals.

The authors have established that from the various 29 types of macrosynoptic weather situations, if they are continuous, which are favourable or unfavourable from the point of view of collecting the moths, moreover how the species investigated react to the change of the weather situations.

Key-words: Hess-Brezowsky's macrosynoptic situations, turnip moth, light trap.

1. Introduction

The principal condition of effective and economical plant-protection taking care of the environment is the reliable prognosis of harmful insects. In order to elaborate a suitable prognosis it is necessary to make simultaneous observations of the time of appearence and the number of individuals, using adequate methods and sampling devices. The light-trap is a wide-spread tool for catch of insects flying at night which kills the insects flown to the artifical light source.

There has been a uniform light-trap network of *Jermy* type in Hungary for

about thirty years which has collected a great amount of valuable data for scientific research. The data representing the activity of insects are influenced by several factors, including the weather. It is easy, therefore, to understand that many entomologists deal with the investigations of the effect of meteorological parameters all over the world. Unfortunately, most of the Hungarian light-trap stations did not observe the meteorological elements. These stations were in general situated remote from meteorological observing stations. We published the effectiveness of catching the most harmful insects by light-traps in earlier papers (*Károssy* and *Nowinszky*, 1987a; *Nowinszky* and *Károssy*, 1986) associated with the *Péczely*'s macrosynoptic weather situations existing in the Carpathian Basin.

In some papers the results of light-trap catches were demonstrated at the time of change of *Péczely*'s type (*Nowinszky* and *Károssy*, 1988; *Károssy* and *Nowinszky*, 1987b). In these publications we searched for the connection between the catching data and the change of 13 types of *Péczely*. The types which seldom occured were eliminated. This method gave much information, but its application was complicated for plant-protecting forecast. In the recent paper a simple method is presented which is easily applicable for plant-protecting forecast. Based on the air flow the 13 situations had been contracted into 6 types and after that the time of their change was investigated (*Károssy et al.*, 1990, 1992).

In the present paper the authors analyse the light-trap catches of turnip moth (*Scotia segetum Schiff.*) in connection with the macrosynoptic weather types of *Hess-Brezowsky* (1977) extended to whole Europe.

2. Material

The determination of macrosynoptic types of *Hess-Brezowsky* had been similarly and subjectively worked out as *Péczely*'s ones, taking into account the circulation conditions of the continent (Europe). The catalogue of *Hess-Brezowsky* (1977) based on baric circumstances of Central Europe, distinguishes 4 zonal, 18 meridional and 7 mixed types of weather situations, maintaining one type for unclassified baric areas. *Bartholy* and *Kaba* (1987) interpreted the *Hess-Brezowsky*'s situations for the whole Atlantic-European area. They analysed a great amount of data processed from 8 Hungarian meteorological stations of 60 years and 18 daily values and determined the *Hess-Brezowsky*'s weather picture for Hungary. The characteristics of these types can be found in literature cited. The codes which were necessary for this investigation, are similarly taken from publication of *Hess-Brezowsky* (1977).

The Hungarian light-trap network is supported by the Forestry Research Institute, the plant-protecting stations and other research organisations. The

uniform light-trap device consists of a 100 W incandescent lamp situated at 2 m above the ground surface and the killing material is chloroform.

During the interval between 1957 and 1976, i.e. through 20 years, 32,100 individuals of turnip moth (*Scotia segetum Schiff.*) were caught by the 61 traps of the network from 20,508 observations and 249 swarmings at 2,647 nights. In our terms, swarming is the time-span of one generation and an observational datum is denoted as the result collected at a single station during one night.

The turnip moth (*Scotia segetum Schiff.*) has two generations yearly and is characterized as a polyphag harmful insect. The first generation in most cases occurs from the beginning of May to the middle of June, while the second one from middle of July to September. This moth is equally dangerous for vegetables, root crops, industrial plants, cereals, leguminouses and ornamental plants.

3. Method

We calculated relative catches (RC) from the obtained data belonging to each collecting stations and generations. This procedure gives us a possibility to compare the results taken at various light-trap stations to each other. The RC is defined as a quotient of the number of individuals caught during a sampling time (a night) and the mean number of a given generation.

The catching data belonging to the same *Hess-Brezowsky*'s 29 types in the evening and morning, have been averaged. After this the significance levels have been computed between them using the *Welch*-test (i.e. an approximate t-test). In cases, if we did not take the macrosynoptic types into account, we applied 1 (the unity) as relative catch value (RC).

In so far as during a two days period the weather types changed, the original 29 situations were sorted into zonal, mixed, meridional, cyclonic or anticyclonic groups on the basis of their circulation characteristics. On this basis we accepted 6 groups, containing the original situations too, as follows:

- Zonal anticyclone: Wa (1), Ws (3), and Ww (4),
- Zonal cyclone: Wz (2),
- Mixed anticyclone: SWa (7), NWa (13), HM (17) and BM (30),
- Mixed cyclone: SWz (8), NWz (14) and TM (25),
- Meridional anticyclone: Sa (5), SEa (9), Na (11), NEa (15), HB (18), HNa (19), HFa (21) and HNFa (23),
- Meridional cyclone: Sz (6), SEz (10), Nz (12), NEz (16), HNz (20), HFz (22), HNFz (24), TB (26), TRM (27) and TRW (28).

The above listed 6 groups can change into 36 possible categories. Continuing the procedure, we have averaged the RC belonging to each variable situation and after this the confidence level was calculated related to the expected value, using the *Welch*-test.

4. Results and discussion

Table 1 contains the averages of RC of the turnip moth (*Scotia segetum Schiff.*) with the number of observations, the confidence levels of the *Hess-Brezowsky* situations which have the same characters in the evening and morning. *Table 2* shows the same data of the changing situations.

The data of Table 1 show that in most case of northern, northwestern and western situations, when the macrosynoptic situations remained unchanged in the evening and in the morning, the number of moths significantly decreased. This phenomenon may be explained by windy and cool weather, which characterizes the night hours generally in these cases. It is conspicuous that high catch can be associated only with four situations, of which three belong to southern or southwestern types. It seems that the continuously existing weather situations are unfavourable for the activity of insects. We obtained similar results earlier in connection with *Péczely*'s situations. From the varying situations in general, the anticyclones are unfavourable, because the character of circulation changes, moreover an anticyclone is followed by a cyclone or a cyclone by anticyclone, respectively.

We have high catch, if a cyclone is succeeded by a cyclone and if a meridional anticyclone is followed by an other one or a meridional cyclone.

The low values of RC are referring in all cases to such a weather situation which cause decresed flying activity of insects. The high values cannot be interpreted unambiguously. The significant changes in environment induce some physiological variations in organism of insects. The life of an imago is short, therefore the unfavourable weather is dangerous as well for individuals as for remaining of whole species. We suggest that an individual, in order to avoid the bad circumstances hindering his normal life, can apply two strategies. The insect shows increased activity which consists of expanded flying, copulation and laying eggs, or passively, hide themself through the unfavourable times. Based on facts discussed above, high RC belongs both to good and bad weather situations.

The present paper is a first one of those investigations, which are associated with the connection between the macrosynoptic situations of *Hess-Brezowsky* and the life circumstances of insects. To the further work, we think it necessary to reveal the characteristics of the behaviours connected with the times of variations of the weather situations. We hope, based on our new results, that a reliable forecast can be established using *Hess-Brezowsky*'s classification all over Europe. In Hungary the *Péczely*'s situations give also good approximation to plant-protection service.

Acknowledgements–The insects caught by light-traps were identified by a team at the Hungarian Museum for Natural Science under the direction of *Lajos Kovács*. The note-books were kindly disposed to us by *András Vojnits*, to whom we express our sincere acknowledgements hereby.

Table 1. The RC of turnip moth (*Scotia segetum Schiff.*) in situations when the *Hess-Brezowsky's* macrosynoptic type has the same character both in the evening and in the morning

Code	H-B situations	Mean of RC	Number of data	Confidence level
	Northern macrosynoptic types			
11	Na	0.757	97	94.45
12	Nz	0.922	463	91.68
19	HNa	0.930	248	-
20	HNz	0.772	376	99.84
18	HB	0.861	384	97.16
	Northwestern macrosynoptic types			
13	NWa	0.972	123	-
14	NWz	0.938	1139	92.68
27	TRM	0.733	240	99.25
	Western macrosynoptic types			
1	Wa	0.948	869	90.05
2	Wz	0.945	2512	96.16
3	Ws	1.020	483	-
	Southwestern macrosynoptic types			
7	SWa	1.295	661	99.90
8	SWz	0.960	471	-
28	TRW	1.210	1084	99.83
4	Ww	1.127	274	-
	Southern macrosynoptic types			
5	Sa	0.746	49	92.70
6	Sz	1.321	18	-
26	TB	1.200	446	96.30
	Southeastern macrosynoptic types			
9	SEa	0.775	66	-
10	SEz	0.812	6	-
	Eastern macrosynoptic types			
21	HFa	0.868	758	98.98
22	HFz	0.969	409	-
23	HNFa	0.895	249	-
24	HNFz	1.061	505	-
	Northeastern macrosynoptic types			
15	NEa	0.999	430	-
16	NEz	1.328	274	98.90
	Types with its center situated above Central-Europe			
17	HM	1.001	1032	-
30	BM	1.104	1055	90.34
25	TM	0.734	142	96.75

Note: The codes are obtained from the paper of *Bartholy* and *Kaba* (1987).

Table 2. The RC of turnip moth (*Scotia segetum Schiff.*) when the *Hess-Brezowsky*'s macrosynoptic types has been changed

Variable situations	RC	Number of data	Confidence level
FROM ZONAL ANTICYCLONE TO			
-zonal anticyclone	-	-	-
-zonal cyclone	0.757	123	97.71
-mixed anticyclone	0.892	188	-
-mixed cyclone	0.813	71	-
-meridional anticyclone	0.714	105	98.67
-meridional cyclone	1.231	103	-
FROM ZONAL CYCLONE TO			
-zonal anticyclone	0.567	106	99.99
-zonal cyclone	-	-	-
-mixed anticyclone	1.031	208	-
-mixed cyclone	1.240	122	90.57
-meridional anticyclone	1.126	24	-
-meridional cyclone	0.916	201	-
FROM MIXED ANTICYCLONE TO			
-zonal anticyclone	1.054	102	-
-zonal cyclone	1.359	276	99.34
-mixed anticyclone	1.058	124	-
-mixed cyclone	1.254	113	-
-meridional anticyclone	0.844	164	93.28
-meridional cyclone	0.976	326	-
FROM MIXED CYCLONE TO			
-zonal anticyclone	1.015	178	-
-zonal cyclone	1.450	72	90.54
-mixed anticyclone	1.073	171	-
-mixed cyclone	1.440	122	-
-meridional anticyclone	1.030	241	-
-meridional cyclone	0.783	120	97.36
FROM MERIDIONAL ANTICYCLONE TO			
-zonal anticyclone	0.543	72	99.75
-zonal cyclone	0.666	12	-
-mixed anticyclone	0.745	179	99.69
-mixed cyclone	1.132	53	-
-meridional anticyclone	1.245	225	94.38
-meridional cyclone	1.267	222	95.70
FROM MERIDIONAL CYCLONE TO			
-zonal anticyclone	1.102	115	-
-zonal cyclone	0.912	219	-
-mixed anticyclone	0.901	222	-
-mixed cyclone	1.182	176	-
-meridional anticyclone	0.833	247	96.59
-meridional cyclone	1.112	491	-

References

Bartholy, J. and *Kaba, M.*, 1987: Statistical analysis and correction of *Hess-Brezowsky*'s macrosynoptic types (in Hungarian). *Meteorológiai Tanulmányok* 57, OMSZ, Budapest.

Hess, P. and *Brezowsky, H.*, 1977: *Katalog der Grosswetterlagen Europas*. Berichte des Deutschen Wetterdienst, 113, 15. Offenbach am Main.

Károssy, Cs. and *Nowinszky, L.*, 1987a: The flying activity of harmful insects at various macrosynoptic situations (in Hungarian). *Légkör 32*, No. 2, 33-35.

Károssy, Cs. and *Nowinszky, L.*, 1987b: Relationship between the amount of turnip moth caught by light-traps and the different macrosynoptic situations (in Hungarian). *Időjárás 91*, 246-252.

Károssy, Cs., *Nowinszky, L.* and *Tóth, Gy.*, 1990: Die Flugaktivität der Saateule (Scotia segetum Schiff.) während des Wechsels von Grosswetterlagen. *Wetter und Leben*, 42, 189-194.

Károssy, Cs., *Nowinszky, L.*, *Tóth, Gy.* and *Puskás, J.*, 1992: Flying activity of the agricultural harmful insects and the connection of macrosynoptic weather types. *Boletin de la Sociedad Geografica de Lima 105*, 57-58.

Nowinszky, L. and *Károssy, Cs.*, 1986: Results of catching of the winter moth (Operophtera brumata L.) by light-traps in different macrosynoptic climatic conditions (in Hungarian). *Kertgazdaság 18*, No. 6, 31-38.

Nowinszky, L. and *Károssy, Cs.*, 1988: The result of light-trapping in connection with macrosynoptic weather situations (in Hungarian). *Növényvédelem 24*, No. 1, 10-17.

INFORMATION

GEDEX: a comprehensive data set on global and regional change

T. Pálvölgyi

Institute for Atmospheric Physics, P.O. Box 39, H-1675 Budapest, Hungary

(Manuscript received 4 March 1993)

Abstract—The primary aim of this paper is to outline the GEDEX (*Greenhouse Effect Detection Experiment*) data set developed for global change analysis. This first issue includes surface, upper air, and/or satellite-derived measurements of temperature, solar irradiance, clouds, greenhouse gases, fluxes, albedo, aerosols, ozone, and water vapour, along with Southern Oscillation Indices and Quasi-Biennial Oscillation statistics. Additionally, the documentation of individual climatic records is discussed briefly and some technical details of handling the data set are also presented. All data incorporated into the GEDEX data set are available on CD-ROMs at the Hungarian Meteorological Service.

Key-words: global change, climate variables monitoring, digital data base.

1. Introduction

During the past 20 years, much attention has been devoted to the potential climatic effects of increasing concentrations of atmospheric greenhouse gases. There are growing evidences that these potential climatic effects could have far-reaching environmental, economic and social consequences, as well. Much of recent study (*IPCC,* 1992) has involved

— climate modelling or empirical analyses attempting to attribute climate change to various atmospheric and astronomical forcing, and
— assemblage and examination of new geological, historical and instrumental data.

From these studies, researchers have gained important new insights into the possible climatic response to the growing level of atmospheric CO_2 and other trace gases, together with a better understanding of the sensitivity of the overall climate system to both human and natural perturbations.

In order to detect the "greenhouse signal" that is indicative of increased concentrations of greenhouse gases, it is imperative to collect observational records that can be used to identify the climate change. For the past century, many climate variables have been measured at a large number of meteorological

stations, mostly at land locations in the Northern Hemisphere. One of the goals of NASA's Climate Data System (NCDS) staff at Goddard Space Flight Center is to provide ready access data and information pertinent to global and regional changes. NCDS has attempted to achieve this goal by providing reports, numerical data packages and other information center products and services.

2. Overview

The *Greenhouse Effect Detection Experiment* (GEDEX) program takes a major step in providing timely data to a multidisciplinary audience of researches, policy-makers, energy and environmental professionals and educators (*GEDEX,* 1992). The GEDEX program is a part of NASA's involvement in the International Space Year (ISY) activities. In preparation for the International Space Year, the *Greenhouse Effect Detection Experiment* organized a workshop to bring together a core group of scientists to share their research and ideas in the area of global climate change. Participants in this workshop, which was designated GEDEX Atmospheric Temperature Workshop, met in Columbia, Maryland, in July 1991 for the purpose of obtaining a measure of progress and recommending actions required to better understand the global atmospheric temperature record and its relationship with climate forcings and feedbacks (*NASA,* 1992).

One of the primary objectives of the workshop was to assemble and document existing data (focusing on temperature) for the analysis of global and regional climate change and to consolidate these selected data sets onto CD-ROMs for distribution nationally and internationally to promote further research. With climate at the focus, NASA's Climate Data System (NCDS) participates and prepares for the acquisition, archiving, implementation, and documentation of data recommended for distribution. NCDS has been designated as the core system for the Goddard Space Flight Center's Distributed Active Archive Center (DAAC) of the Earth Observing System Data and Information System (EOSDIS), and in this role will continue to update GEDEX-relevant data sets. All data will remain in the Goddard DAAC (NCDS) and will be updated whenever new releases are made available. Subsequent updates will therefore be made available in an ongoing manner to the climate user community. More than 60 data sets were identified by workshop participants for inclusion, yielding nearly 1 gigabyte of data for this first 2-disk set of CD-ROMs. Most participants contributed data and helped in the preparation of the standard documentation for each data set proposed for CD-ROM. Each data set was verified by the NCDS after it was transformed into a standard format (the Common Data Format [CDF] to allow for the use of a single set of software tools to access the data on disks). Iterations of the detailed documentation and extensive verification with data producers ensure that the data are reproduced

as received from data producers. The data producers cooperated fully with this essential effort.

3. *Contents*

Although the focus of the first GEDEX workshop was on temperature, other parameters such as solar irradiance, atmospheric constituents, cloud, and radiation budget data, which affect the temperature record, were considered essential components of the data base. The GEDEX data sets include surface, upper air, and/or satellite-derived measurements of temperature, solar irradiance, clouds, greenhouse gases, fluxes, albedo, aerosols, ozone, and water vapour, along with Southern Oscillation Indices and Quasi-Biennial Oscillation statistics. Many of the data sets provide global coverage. The spatial resolutions vary from zonal to 2.5 degree grids. Temporal coverage also varies. Some surface station data sets cover more than 100 years, while most of the satellite-derived data sets cover only the most recent 12 years. Temporal resolution, for most data sets, is monthly (*Table 1*).

Table 1. Basic characteristics of some selected GEDEX data sets

	Spatial coverage	Spatial resolution	Temporal coverage	Temporal resolution
Surface temperature	global	2.5° grid	> 100 years	monthly
Upper air temperature	Northern Hemisphere	zonal	35 years	monthly
Cloudiness	global	2.5° grid	5 years	monthly
Radiation budget	global	5° grid	9 years	monthly
Solar irradiance	single site (Mauna Loa)	-	32 years	daily
CO_2 concentration	certain sites (32 stations)	-	10-25 years	monthly
CH_4 concentration	certain sites (21 stations)	-	9-13 years	monthly
N_2O concentration	Northern Hemisphere	zonal	7 years	seasonal
Total ozone	certain sites (85 stations)	-	22 years	monthly

3.1 Surface temperature

The basic surface station temperature data set from NCDC/NCAR contains monthly temperature and precipitation values and is subdivided by continent. A few records dated from as early as 1738, and modern station data extend

through 1989. Other surface temperature anomaly data sets containing monthly gridded values were provided by the University of East Anglia Climate Research Unit (*Jones et al.*, 1991), and by the Goddard Institute for Space Studies (*Hansen* and *Lebedeff*, 1988). Zonal and station temperature data are included from the Russia's State Hydrologic Institute (*Vinnikov et al.*, 1990). These data sets extend over 100 years of record. Gridded 2.5 degree monthly sea-surface temperature data and anomalies as calculated by NOAA's Climate Analysis Center also reside on this disk. These SST values are from AVHRR sensors on NOAA polar orbiters and are blended with ship and buoy data. Investigating the effect of the El Niño/Southern Oscillation (ENSO) on the temperature anomaly record, may be done with the data set provided by the University of East Anglia's Climate Research Unit containing the Southern Oscillation Index calculations, along with the Tahiti and Darwin mean sea level pressures from which they are derived.

3.2 Upper air temperature

NCDC/NCAR contributed comprehensive monthly station rawinsonde data (*Spangler* and *Jenne*, 1990). Both temperature and humidity profiles are included in this data set. Another upper air temperature data set was produced by NOAA ARL (*Angell*, 1988). It contains seasonal zonal temperature deviations from rawinsonde data around the world. *Angell* also provided Quasi-Biennial Oscillation temperature and zonal wind data at 50, 30, and 10 hPa. Marshall Space Flight Center provided more than 12 years of mid-tropospheric temperature and anomaly data from the TIROS Operational Vertical Sounder Microwave Sounding Unit (TOVS-MSU), flown on NOAA polar orbiters (*Spencer* and *Christy*, 1992). Stratospheric temperature data were provided by NCAR (*Labitzke* and *van Loon*, 1991). Although these data are only available for the Northern Hemisphere, they provide a valuable monthly zonal product for the years 1957 to 1991. In addition, profiles of meteorological data from NMC were provided at 1 km intervals for the Stratospheric Aerosol and Gas Experiment (SAGE II) time period .

3.3 Solar irradiance and transmission

Solar transmission and surface-measured irradiance data were compiled by NOAA Climate Monitoring and Diagnostics Laboratory (CMDL). The daily solar transmission indices, given from the Mauna Loa Observatory, begin in 1958 and continue through 1990 (*Reid*, 1991). The hourly solar irradiance data make up a rare collection of solar data collected at the surface from 1976 to 1989 at selected sites. NASA Goddard Space Flight Center provided solar irradiance data from the Nimbus-7 Earth Radiation Budget (ERB) instrument, and Langley Research Center offered the solar irradiance data from NOAA-9,

NOAA-10, and ERBS. Jet Propulsion Laboratory has collaborated with the NCDS staff over the years in making 9 years of solar irradiance data from the Solar Maximum Mission's ACRIM sensor available to users online (*Willson* and *Hudson,* 1991). From the Dominion Radio Astrophysical Observatory (DRAO) (formerly Ottawa) 2800 MHz radio flux data are also available on the disk with observed, absolute, and adjusted variables from 1947 to the present.

3.4 Radiation budget and clouds

Langley Research Center provided the combined Earth Radiation Budget Experiment's (ERBE S4) satellite gridded products, including the scanner data at 2.5 degree resolution and the wide-field-of-view monthly averages. NASA GISS suggested and subsequently provided a comprehensive subset of the *International Satellite Cloud Climatology Project's* (ISCCP) monthly cloud products at 2.5 degree resolution. ISCCP also assisted in the review and verification of those data worked closely with the staff in the validation of data on the disk from the Earth Radiation Budget instrument on board Nimbus-7. Data from the wide-field-of-view sensor span the period 1978 to 1987 and are monthly in temporal resolution and approximately 4.5 by 5 degrees in spatial resolution. Data are derived from NOAA Polar Orbiting satellites using TOVS-HIRS and TOVS-MSU sensors.

3.5 Atmospheric constituents

The Carbon Dioxide Information Analysis Center (CDIAC), Department of Energy, is the source providing carbon dioxide and methane values spanning the geological record (through ice core techniques) and more recent values collected by NOAA from flask sampling and continuous monitoring techniques (*TRENDS*, 1990). NOAA ARL also contributed seasonal layer ozone data from Umkehr sounding and ozonesondes from 1957 to 1990, and total ozone from Dobson spectrophotometers for the period 1967 to 1989 (*Stolarski et al.*, 1991). NASA's Langley Research Center worked closely with NCDS in providing ozone, nitrogen dioxide, and aerosol data from the Atmospheric Explorer Mission's SAGE I instrument, and aerosol, ozone, water vapor, and nitrogen dioxide data from the Earth Radiation Budget Satellite's (ERBS) SAGE II instrument beginning with data from the November 1984 launch through 1991 (*McCormick et al.*, 1992).

3.6 Satellite-based data

The satellite-based data sets are those from Solar Maximum Mission's ACRIM instrument, the Nimbus-7 Earth Radiation Budget instrument, the Atmospheric Explorer Mission's SAGE I sensor, the Earth Radiation Budget

Satellite's SAGE II sensor, the NOAA polar orbiter TOVS-HIRS and TOVS-MSU instruments, the Earth Radiation Budget Experiment (NOAA-9, NOAA-10, and ERBS sensors), and AVHRR, MIR and VAS sensors on NOAA Polar Orbiters, GOES, METEOSAT, and GMS satellites.

4. Documentation

Each record of the data set is supplied by detailed catalogues containing fourteen items (with standardized subheadings). These give information on the type of the data, spatial and temporal characteristics, instrument description, data processing sequence, quality assessment, contacts for data production, output products and availability, data access, archive information, references, related data sets, summary/sample, and a final item for notes (*Appendix A*). Much of the information was provided by the data producers, however NCDS staff members supplemented this information and standardized presentation. As a result, specific details can be readily located through the table of contents. In addition to the detailed catalogues directly linked with the data sets held on the CD-ROM, ancillary catalogues that are closely related to the resulting products are included. These catalogues give descriptions of the products from which many of the data sets are derived and include:

ERB:	Nimbus-7 Earth Radiations Budget
ERBE	Earth Radiation Budget Experiment
AVHRR	Advanced Very High Resolution Radiometer
SAGE I	Stratospheric Aerosol and Gas Experiment I
SAGE II	Stratospheric Aerosol and Gas Experiment II
TOVS HIRS	TIROS Operational Vertical Sounder High-resolution. Infrared Radiometer
TOVS MSU	TIROS Operational Vertical Sounder Microwave Sounding Unit
TOVS SSU	TIROS Operational Vertical Sounder Stratospheric Sounding Unit
VISSR	Visible and Infrared Spin Scan Radiometer
VAS	VISSR Atmospheric Sounder

In addition, the detailed documentation also contains descriptions of satellite sensors and the products from which the geophysical parameters of this data base are derived. Among these are AVHRR, TOVS, VAS, VISSR, ERB, ERBE, SAGE I, and SAGE II.

5. Technical background

All of the data incorporated into GEDEX are stored in binary files, written in the NASA/GSFC Common Data Format (CDF). Common Data Format is a

conceptual data abstraction for storing multi-dimensional data sets widely used in the climate research community. The CDF program allows direct access to related variable data values. The data values of up to 27 variables may be displayed at once (the CDF can have more variables but only 27 may be viewed at any one time). The data value for each variable at a given record/index location within the CDF conceptual view is displayed. The user can "walk" from one record/index location to another sequentially (in any "direction") or a particular record/index location can be "jumped" to directly. Variable values may also be used to directly "jump" to a record/index location. They are network-encoded for portability and are written with the single file option for simplicity.

The directory hierarchy is the same for both CD-ROMs. There are five major subdirectories on the discs, as given below:

[DATA] The data sets (in Common Data Format) containing the actual data sets (with file name extension CDF). A separate file CDF.DOC in the DOCUMENT subdirectory serves as references to the format of the data and supporting software.

[DETAILED] Detailed catalogues for the individual data sets and sensors describing comprehensive information about the data sets on the disk. Files are in ASCII: each line of text delimited by a carriage return (ASCII 13) and a line feed (ASCII 10).

[DOCUMENT] Overall documentation for the CD-ROM (ASCII text files of documentation about the disk structure, data formats and accompanying software).

[INDEX] Various tables of data describing the data sets that are suitable for import into a database management system. This contains comma-delimited index files which may be imported into a database program, in order to facilitate searches of the data present on the disk.

[SOFTWARE] Utility programs for manipulating data in CDF under MS-DOS, DEC VAX or UNIX operating systems, along with the portable CDF software library for working with the data sets on the disk. There are separate directories for MS-DOS, HP-UX, SunOS, IRIX and VMS utilities, as well as a CDF subdirectory which contains the complete CDF distribution set of files.

[SUMMARY] Summary documentation required by the access software to provide standard information for each individual data set.

There are several files associated with each data set. The kind of information stored in a file can be inferred from the extension on the file name:

[CDF] The data, formatted to CDF v2.1 as network-encoded, single

file data sets. These are all located in the DATA subdirectory.

[DET] A text file, containing the NCDS Detailed Catalogue associated with the data set. All of these files are located in the DETAILED subdirectory.

[SUM] A text file, containing summary information about the data set. All of these files are located in the SUMMARY subdirectory.

Since several data sets may share a single detailed catalogue, the file PRODUCTS.LIS (in the SUMMARY subdirectory) gives a tabular listing of the name of the data file, a brief description of the data set and the name of the associated detailed catalogue, as well.

6. Conclusions

Activities in the scientific and policy-making communities have been stimulate by public concerns related to global environmental issues. Recognition is growing that it is increasingly important to have valid and reliable data at hand to develop effective policies related to these issues. The most promising potential key research areas for the application of GEDEX data sets are

- detection of enhanced greenhouse effect based on evaluation and prediction of climate variability and trends on various space and time scale,
- parameterization of climate processes, validation and verification of climate models,
- investigation of spatial distribution and life cycle of climatic fluctuations and teleconnections arising on decadal time scale,
- assessment of global and regional climate scenarios based on analogue method,
- renewed climatological database into a limited area model,
- various applications in the satellite climatology

It can be concluded that such data sets are essential to analyse and evaluate the magnitude of environmental problems that have global or regional implications.

References

Angell, J.K, 1988: Variations and trends in tropospheric and stratospheric global temperatures, 1958-1987. *J. Clim. 1*, 1296-1313.

GEDEX, 1992: *Booklet on the greenhouse effect detection experiment* (eds.: L.M. Olsen and A. Warnock), NASA Goddars Space Flight Center, Greenbelt, U.S.A.

Hansen, J. and *Lebedeff, S.*, 1988: Global surface air temperatures: update through 1987. *Geophys. Res. Lett. 15*, 323-326.

IPCC, 1992. *Climate Change: The Supplementary Report to the IPCC Scientific Assessment* (eds.: J.T. Houghton, B.A. Callander and S.K. Varney). Cambridge University Press, Cambridge, 192 pp.

Jones, P.D., Wigley, T.M.L. and *Farmer, G.*, 1991: Marine and land temperature data sets: a comparison and a look at recent trends. In *Greenhouse Gas Induced Climate Change: a Critical Appraisal of Simulations and Observations* (ed.: M.E. Schlesinger). Elsevier, Amsterdam, pp. 153-172.

Labitzke, K. and *van Loon, H.*, 1991: Some complications in determining trends in the stratosphere. *Adv. Space Res. 11*, (3)21-(3)30.

McCormick, M.P., Veiga, R.E. and *Chu, W.P.*, 1992: Stratospheric ozone profile and total ozone trends derived from the SAGE I and SAGE II data. *Geophys. Res. Lett. 19*, 269-272.

NASA, 1992: *The Detection of Climate Change due to the Enhanced Greenhouse Effect* (A synthesis of findings based on the GEDEX atmospheric temperature workshop, ed.: R.A. Schiffer). NASA Goddard Space Flight Center, Greenbelt, U.S.A.

Reid, G.C., 1991: Solar total irradiance variations and the global sea surface temperature record. *J. Geophys. Res. 96*, 2835-2844.

Spangler, W.M. and *Jenne, R.L.*, 1990: *World Monthly Station Climatology*. CDT documentation, NCAR, Boulder, U.S.A.,

Spencer, R.W. and *Christy, J.R.*, 1992: Precision and radiosonde validation of satellite gridpoint temperature anomalies. *J. Clim.* (in press).

Stolarski, R.S., Bloomfield, P., McPeters, R.D. and *Herman, J.R.*, 1991: Total ozone trends deduced from NIMBUS 7 TOMS data. *Geophys. Res. Lett. 18*, 1015-1018.

TRENDS, 1990: *A Compendium of Data on Global Change*. Oak Ridge National Laboratory, Oak Ridge, U.S.A.

Vinnikov, K.Ya., Groisman, P.Ya. and *Lugina, K.M.*, 1990: Empirical data on contemporary global climate changes (temperature and precipitation). *J. Clim. 3*, 662-677.

Willson, R.C. and *Hudson, H.S.*, 1991: The Sun's luminosity over a complete solar cycle. *Nature 351*, 547-560.

APPENDIX A Detailed documentation of GEDEX data sets

1. TYPE OF DATA
   - 1.1 Parameter/Measurement
   - 1.2 Unit of Measurement
   - 1.3 Data Source
   - 1.4 Data Set Identification

2. SPATIAL CHARACTERISTICS
   - 2.1 Spatial Coverage
   - 2.2 Spatial Resolution

3. TEMPORAL CHARACTERISTICS
   3.1 Temporal Coverage
   3.2 Temporal Resolution

4. INSTRUMENT DESCRIPTION
   4.1 Mission Objectives
   4.2 Key Satellite Flight Parameters
   4.3 Principles of Operation
   4.4 Instrument Measurement Geometry

5. DATA PROCESSING SEQUENCE
   5.1 Processing Steps and Data Sets
   5.2 Derivation Techniques/Algorithms
   5.3 Special Corrections/Adjustments
   5.4 Processing Changes

6. QUALITY ASSESSMENT
   6.1 Data Validation by Producer
   6.2 Confidence Level/Accuracy Judgement
   6.3 Usage Guidance

7. CONTACTS FOR DATA PRODUCTION INFORMATION

8. OUTPUT PRODUCTS AND AVAILABILITY
   8.1 Tape Products
   8.2 Film Products
   8.3 Other Products

9. DATA ACCESS
   9.1 Archive Identification
   9.2 Procedures for Obtaining Data
   9.3 NCDS Status/Plans

10. CONTACTS FOR ARCHIVE/DATA ACCESS INFORMATION

11. REFERENCES
   11.1 Satellite/Instrument/Data Processing Documentation
   11.2 Journal Articles and Study Reports
   11.3 Archive/DBMS Usage Documentation

12. RELATED DATA SETS

13. SUMMARY/SAMPLE

14. NOTES

BOOK REVIEW

Atlas of Paleoclimates and Paleoenvironments of the Northern Hemisphere. Late Pleistocene–Holocene (published by the Geographical Research Institute, Hungarian Academy of Sciences, Budapest, on behalf of the International Union for Quaternary Research; edited by *Frenzel, B., M. Pécsi* and *A.A. Velichko*; explanatory text edited by *L. Bassa* and *O. Soffer*; Published by Fisher Verlag, Stuttgart–Jena–New York, Geographical Res. Inst., Hung. Acad. Sci., Budapest, 1992; 153 pages, 35 large size color maps.)

The production of this important publication was sponsored by the Executive Committee of the International Union for Quaternary Research (INQUA), the Hungarian Academy of Sciences, the Academy of Sciences and Literature (Mainz), the Federal Ministry of Research and Technology (Bonn) and the Enkidu Foundation (Berne–Tübingen). The contributing institutions were: the Geographical Research Institute of the Hungarian Academy of Sciences, the Research Project Group "Terrestrial Paleoclimatology" of the Academy of Sciences and Literature (Mainz) and the Laboratory of Paleogeography of the Academy of Sciences of the USSR. Contributions from 62 authors (mainly from Germany and the USSR) were compiled and carefully edited. In addition to the contributors, 16 more scientists were involved in the revision of the maps. The number of references (353) also gives an idea of the magnitude of the undertaking. The cartography and printing was done by the Geographical Research Institute of the Hungarian Academy of Sciences.

In the atlas altogether 9 maps deal with the *Last Interglacial* (about 120,000 yr B.P.), 5 maps with the *interstadial of the last glaciation* (about 35,000 to 25,000 yr B.P.), 11 maps with the *maximum cooling period* of the last glaciation (about 20,000 to 18,000 yr B.P.), 2 maps with the *upper pleniglacial* of the last glaciation (about 24,000 to 12,000 yr B.P.), and finally 8 maps with the *Holocene* (between 7,000 and 5,500 yr B.P.).

The *Quaternary* period (Pleistocene and Holocene) comprises the last 2 million years of the history of the Earth. This was the time span of the emergence of early man, whose evolution was greatly influenced by climatic changes. The *International Union for Quaternary Research* (INQUA) was established in the early thirties in recognition of the particular importance of this period.

Some 14 years ago INQUA has established its *Commission on Paleogeographic Atlas of the Quaternary* in order to compile and publish the results of the wide ranging research works on the spatial and temporal paleogeographical changes on the Northern Hemisphere during the *last climatic macrocycle* (last 130,000 years).

It is generally assumed that the above mentioned last climatic macrocycle is a typical example of the climatic cycles which followed each-other during the 2 million years of the Quaternary. A detailed analysis of the last climatic macrocycle is considered, therefore, a relevant contribution to the deeper understanding of the climatic history of the whole period.

The *climatic reconstructions* contained in the atlas are based on different approaches and methods, consequently they are not always in full agreement. Nevertheless, these reconstructions allow some conclusions about the hydrothermal regime of the Northern Hemisphere and provide an idea about various environmental responses, such as conditions and distribution of vegetation, permafrost and hydrology.

During the last 130,000 years the Earth experienced at least twice periods of pronounced warmer climates (during the Last Interglacial and during the Holocene climatic optimum), and two phases of cold climates (the interstadial complex and the pleniglacial phase).

In connection with paleoclimatic reconstructions and mapping two major types of difficulties are usually encountered: (*a*) *the difficulties in establishing correlations (synchronism) between events occurring in different regions of the globe, and (b) the synthesis of reconstructions obtained by different methods.*

As regards the Holocene, dating is easy by radiocarbon analysis, or by dendrochronology. Thus, for the Holocene climatic optimum no major problems were encountered in correlating the events that occurred in various parts of the globe. It seems, it was a bit tricky to deal with the Last Interglacial, and it was quite difficult to analyse the two cold periods mentioned above. Because of such difficulties it was decided in some cases to show different reconstructions rather than trying to give preference to a single one.

The climatic reconstructions in the atlas are often based on comparing former vegetation communities and soil types to their nearest modern equivalents. This approach, however, is sometime complicated by the fact that neither during the Last Interglacial, nor during the Holocene had all plant and animal taxa (categories of species) sufficient time to occupy their climate-controlled optimal distribution areas.

Nevertheless, it was possible to focus on those phases which could be shown to be synchronous directly by biostratigraphical methods. To mention some examples: the *Eem* epoch of Western Europe could be correlated with the *Mikulino Interglacial* of Eastern Europe, and with marine sequences of the North Sea, Baltic Sea, and Norwegian Sea. Also some episodes of the Eemian pollen sequence are recorded in the Oxygen Isotope Substage 5e, which is also the case for the *Sangamon Interglacial* of Western North America.

One of the very interesting points in these reconstructions is the finding that during the *Last Interglacial* an apparently *warmer climate* (2 to 3°C warmer than today) was accompanied—almost everywhere—by an *increased humidity*. This conclusion *contradicts current GCM model-predictions* which mostly

suggest a greenhouse induced climatic warming accompanied by increasing aridity in presently dry regions (and also in that part of Europe which extends between 35 and 50°N). This point is mentioned just as an example of the kind of intriguing questions which may provide ample food for speculations in connection with the 35 maps of the atlas and the findings of the climatic reconstructions which are described in the text.

In conclusion I would like to stress the importance of this publication. As we can see, nowadays an increasing number of textbooks and publications deal with climatic change, and they usually contain at least brief summaries of paleoclimatic information. Probably I'm not the only one who used to be confused and frustrated by such summaries, which try to provide a simplified picture of a rather chaotic subject. Isolated and sporadic reconstructions of past climates make seldom sense in explaining global climate change chronologies. The only way to somewhat ease this problem is to go meticulously through the hard work of establishing correlations between paleoclimatic events that occurred in different parts of the globe and to produce maps like the ones presented in this atlas.

R. Czelnai

A. Carbonneau, C. Riou, D. Guyon, J. Riom and *C. Schneider*: **Agrometeorology of the Vine Crop** (in French). Centre Commune de Recherche, Commission des Communautés Européennes, 1992, pp. 1–165.

This publication of the *Commission of the European Communities* (CEC) provides an inventory of available information on the agrometeorology of vine, based on a review of literature and experts' opinions. It contains two main parts: the first (and main) part, dealing with the *agrometeorology of vine*, and the second part, containing a preliminary study on *monitoring of vine-lands by remote sensing techniques*.

The flow of accurate and timely information on the state of crop cultures is a vital component in market economies. The Commission of the European Communities, considering the necessity of obtaining such early information, established a *pilot project* for the introduction of remote sensing in the agricultural statistical information system of the Community. It was also a requirement that the whole methodology should be developed in a way suitable for generating a meteorological input in a compatible form for the standard Geographical Information System of CEC.

Although, it was fully recognized that for an adequate early (or advance) information system primarily remote sensing techniques would be required, it was also clear that such techniques were not yet sufficiently developed for the

monitoring of the vine crop. Therefore, it was concluded that remote sensing techniques will have to be applied in combination with quite sophisticated agrometeorological modelling techniques.

Thus the first part of the work done under the project aimed at the development of *agrometeorological models* appropriate for a regional monitoring of the state of the cultures and for the quantitative prediction of crops. The sub-titles in this first part of the publication are: The biological cycle of vine and the climatic parameters; Mesoclimate and microclimate of vine; Climate and growth; The climatic influences on the photosynthesis; Climatic interactions with the organism of the entire plant and its productivity; Methods of viticultural harvest-prediction. These chapters together provide a concise package of very useful information.

The second part of the publication, as already indicated above, contains a *preliminary study on the application of remote sensing techniques* for the monitoring of vine-lands. This is a very sobering report, from which we can see how little has been done so far in the area of remote sensing studies of the vine crop.

The main reason is that the vineyards do not behave well on LANDSAT or even SPOT images. A relatively large percentage of the surface "seen" by a satellite is the bare soil between the rows of vines. The spatial resolution of even the HRV sensor of the SPOT satellite (which is the best at the moment) is quite insufficient to tackle this problem and to provide useful information in a direct fashion.

Two ways were, however, considered for the possible enhancement of such satellite information: the use of multi-temporal series of images, and the application of stereo-radiometric methods (which provide a chance for evaluating the differences between the images taken under different angles relating to the rows of the vine plants). The report only gives us a hint on the possible future direction of research into these possibilities.

R. Czelnai

ATMOSPHERIC ENVIRONMENT

an international journal

To promote the distribution of Atmospheric Environment *Időjárás* publishes regularly the *contents* of this important journal. For further information the interested reader is asked to contact *Dr. P. Brimblecombe,* School for Environmental Sciences, University of East Anglia, Norwich NR 7TJ, U.K.

Volume 27A Number 4 1993

Volume 27A Number 5 1993

D. Grosjean, E. Grosjean and *E.L. Williams II*: Fading of artists' colorants by a mixture of photochemical oxidants, 765-772.

E.Yu. Bezuglaya, A.B. Shchutskaya and *I.V. Smirnova*: Air pollution index and interpretation of measurements of toxic pollutant concentrations, 773-779.

R. Bianconi and *M. Tamponi*: A mathematical model of diffusion from a steady of short duration in a finite mixing layer, 781-792.

Technical Note

M.T. Odman and *A.G. Russell*: A nonlinear filtering algorithm for multidimensional finite element pollutant advection schemes, 794-799.

Volume 27A Number 6 1993

European Monitoring and Evaluation Program Workshop on the Combined Analysis of Measurements and Model Results with Special Emphasis on NO_x/VOC/Oxidants

D.M. Whelpdale: Foreword, 805.

J. Padro: Seasonal contrasts in modelled and observed dry deposition velocities of O_3, SO_2 and NO_2 over three surfaces, 807-814.

N.Z. Heidam: Nitrogen deposition to the Baltic Sea: experimental and model estimates, 815-822.

K. Kemp: A multi-point receptor model for long-range transport over southern Scandinavia, 823-830.

J. Schaug, T. Iversen and *U. Pedersen*: Comparison of measurements and model results for airborne sulphur and nitrogen components with kriging, 831-844.

Z. Zlatev, J. Christensen and *A. Eliassen*: Studying high ozone concentrations by using the Danish Eulerian model, 845-865.

H. Hass, A. Ebel, H. Feldmann, H.J. Jakobs and *M. Memmesheimer*: Evaluation studies with a regional chemical transport model (EURAD) using air quality data from the EMEP monitoring network, 867-887.

T. Iversen: Modelled and measured transboundary acidifying pollution in Europe–verification and trends, 889-920.

D. Simpson: Photochemical model calculations over Europe for two extended summer periods: 1985 and1989. Model results and comparison with observations, 921-943.

A. Sirois: Temporal variation of sulphate and nitrate concentration in precipitation in eastern North America: 1979-1990, 945-963.

N.C. Treloar: Source types in Canadian precipitation chemistry, 965-974.

R.L. Dennis, J.N. McHenry, W.R. Barchet, F.S. Binkowski and *D.W. Byun*: Correcting RADM's sulfate underprediction: discovery and correction of model errors and testing the corrections through comparisons against field data, 975-997.

J.E. Pleim and *J.K.S. Ching*: Interpretive analysis of observed and modeled mesoscale ozone photochemistry in areas with numerous point sources, 999-1017.

A.M. Macdonald, C.M. Banic, W.R. Leaitch and *K.J. Puckett*: Evaluation of the Eulerian Acid Deposition and Oxidant Model (ADOM) witn summer 1988 aircraft data, 1019-1034.

C.S. Davis: Wet deposition monitoring and modelling in New Brunswick–an area dominated by wet deposition due to long-range transport, 1035-1049.

Volume 27A Number 7 1993

S.E. Pitovranov, V.V. Fedorov and *L.L. Edwards*: Optimal sampler siting for atmospheric tracer experiments taking into account uncertainties in the wind field, 1053-1059.

T. Kitada, P.C.S. Lee and *H. Ueda*: Numerical modeling of long-range transport of acidic species in association with meso-β-convective-clouds across the Japan Sea resulting in acid snow over coastal Japan–I. Model description and qualitative verifications, 1061-1076.

T. Kitada and *P.C.S. Lee*: Numerical modeling of long-range transport of acidic species in association with meso-β-convectice-clouds across the Japan Sea resulting in acid snow over coastal Japan–II. Results and discussion.

J.A. Adedokun and *B. Holmgren*: Acoustic sounder Doppler measurement of the wind fields associated with a mountain stratus transformed into a valley fog: a case study.

K.E. Fekete and *L. Gyenes*: Regional scale transport model for ammonia and ammonium, 1099-1104.

M. Schatzmann, W.H. Snyder and *R.E. Lawson Jr.*: Experiments with heavy gas jets in laminar and turbulent cross-flows, 1105-1116.

G. Zappia, C. Sabbioni and *G. Gobbi*: Non-carbonate carbon content on black and white areas of damaged stone monuments, 1117-1121.

R. Sequeira: On the mass-transfer of major salt constituents from sea water to atmospheric precipitation, 1123-1129.

J.-M. Lin, G.-C. Fang, T.M. Holsen and *K.E. Noll*: A comparison of dry deposition modeled from size distribution data and measured with a smooth surface for total particle mass, lead and calcium in Chicago, 1131-1138.

J.F. Pankow: A simple box model for the annual cycle of partitioning of semi-volatile organic compounds between the atmosphere and the Earth's surface, 1139-1152.

J.W. Erisman, A.H. Versluis, T.A.J.W. Verplanke, D. de Haan, D. Anink, B.G. van Elzakker, M.G. Mennen and *R.M. van Aalst*: Monitoring the dry deposition of SO_2 in the Netherlands: results for grassland and heather vegetation, 1153-1161.

NOTES TO CONTRIBUTORS

The purpose of *Időjárás* is to publish papers in the field of theoretical and applied meteorology. These may be reports on new results of scientific investigations, critical review articles summarizing current problems in certain subject, or shorter contributions dealing with a specific question. Authors may be of any nationality but papers are published only in English.

Papers will be subjected to constructive criticism by unidentified referees.

* * *

The manuscript should meet the following formal requirements:

Title should contain the title of the paper, the names(s) of the author(s) with indication of the name and address of employment.

The title should be followed by an *abstract* containing the aim, method and conclusions of the scientific investigation. After the abstract, the *key-words* of the content of the paper must be given.

Three copies of the manuscript, typed with double space, should be sent to the Editor-in-Chief: *P.O. Box 39, H-1675 Budapest,* Hungary.

References: The text citation should contain the name(s) of the author(s) in Italic letter or underlined and the year of publication. In case of one author: *Miller* (1989), or if the name of the author cannot be fitted into the text: *(Miller,* 1989); in the case of two authors: *Gamov* and *Cleveland* (1973); if there are more than two authors: *Smith et al.* (1990). When referring to several papers published in the same year by the same author, the year of publication should be followed by letters a,b etc. At the end of the paper the list of references should be arranged alphabetically. For an article: the name(s) of author(s) in Italics or underlined, year, title of article, name of journal, volume number (the latter two in Italics or underlined) and pages. E.g. *Nathan, K. K.,* 1986: A note on the relationship between photosynthetically active radiation and cloud amount. *Időjárás 90,* 10-13. For a book: the name(s) of author(s), year, title of the book (all in Italics or underlined with except of the year), publisher and place of publication. E.g. *Junge, C. E.,* 1963: *Air Chemistry and Radioactivity.* Academic Press, New York and London.

Figures should be prepared entirely in black India ink upon transparent paper or copied by a good quality copier. A series of figures should be attached to each copy of the manuscript. The legends of figures should be given on a separate sheet. Photographs of good quality may be provided in black and white.

Tables should be marked by Arabic numbers and provided on separate sheets together with relevant captions. In one table the column number is maximum 13 if possible. One column should not contain more than five characters.

Mathematical formulas and *symbols:* non-Latin letters and hand-written marks should be explained by making marginal notes in pencil.

The final text should be submitted both in manuscript form and on *diskette.* Use standard 3.5" or 5.25" DOS formatted diskettes for this purpose. The following word processors are supported: WordPerfect 5.1, WordPerfect for Windows 5.1, Microsoft Word 5.5, Microsoft Word for Windows 2.0. In all other cases the preferred text format is ASCII.

* * *

Authors receive 30 *reprints* free of charge. Additional reprints may be ordered at the authors' expense when sending back the proofs to the Editorial Office.

Published by the Hungarian Meteorological Service

Budapest, Hungary

INDEX: 26 361

HU ISSN 0324-6329